2-P

NASA TECHNICAL MEMORANDUM

NASA TM X-64698
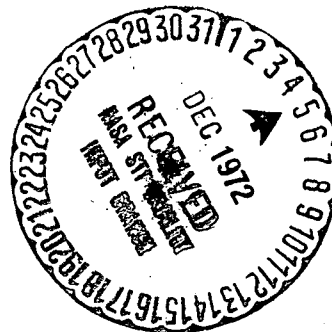
THE PSEUDONOISE TEST SET: COMMUNICATION SYSTEM'S PERFORMANCE EVALUATION BASED UPON RMS ERROR TESTING

By G. R. Wallace
Astrionics Laboratory

S. S. Gussow, W. E. Salter,
and G. D. Weathers
Sperry Rand Corporation

July 1972

NASA

George C. Marshall Space Flight Center
Marshall Space Flight Center, Alabama

1. REPORT NO. TM X- 64698	2. GOVERNMENT ACCESSION NO.	3. RECIPIENT'S CATALOG NO.
4. TITLE AND SUBTITLE The Pseudonoise Test Set: Communication System's Performance Evaluation Based Upon RMS Error Testing		5. REPORT DATE July 1972
		6. PERFORMING ORGANIZATION CODE
7. AUTHOR(S) G.R. Wallace, S.S. Gussow*, W.E. Salter*, and G.D. Weathers*		8. PERFORMING ORGANIZATION REPORT #
9. PERFORMING ORGANIZATION NAME AND ADDRESS George C. Marshall Space Flight Center Marshall Space Flight Center, Alabama 35812		10. WORK UNIT, NO.
		11. CONTRACT OR GRANT NO.
		13. TYPE OF REPORT & PERIOD COVERED
12. SPONSORING AGENCY NAME AND ADDRESS National Aeronautics and Space Administration Washington, D.C. 20546		Technical Memorandum
		14. SPONSORING AGENCY CODE

15. SUPPLEMENTARY NOTES

Prepared by Astrionics Laboratory, Science and Engineering
*Employed by Sperry Rand Corporation

16. ABSTRACT

A pseudonoise (PN) test set has been built to provide a relatively easy means of accurately determining the end-to-end rms error introduced by a communication system when subjected to wideband data. It utilizes a filtered pseudorandom sequence generator as a wideband data source, providing a convenient means for digitally delaying the input reference signal for comparison with the "distorted" test communication system output. In addition to providing a means to measure the end-to-end rms error and the average delay of a communication system, the PN test set also provides a means to determine the tested system's impulse response and correlation function. The theory of PN testing is discussed in detail along with the most difficult aspects of implementation, the building of matched filter pairs. Both analytical and empirical results are reported which support the contentions that this is an accurate and practical way to acquire figures of merit for complete communication systems.

17. KEY WORDS communication systems testing pseudonoise testing filter network sensitivity rms error	18. DISTRIBUTION STATEMENT Unclassified – Unlimited

19. SECURITY CLASSIF. (of this report) Unclassified	20. SECURITY CLASSIF. (of this page) Unclassified	21. NO. OF PAGES 75	22. PRICE $3.00

MSFC - Form 3292 (May 1969)

TABLE OF CONTENTS

LIST OF ILLUSTRATIONS

LIST OF ILLUSTRATIONS (Concluded)

THE PSEUDONOISE TEST SET: COMMUNICATION SYSTEM'S PERFORMANCE EVALUATION BASED UPON RMS ERROR TESTING

I. INTRODUCTION

Until recently, the usual practice in end-to-end testing of communication systems has been to feed simple, deterministic signals into the system being tested and note the response. The response was then compared with a delayed and amplitude scaled version of the input signal to enable one to determine the distortion caused by the system and, thus, establish a system figure of merit. Unfortunately, most communication systems experience complex input signals and true simulations of system inputs are difficult to obtain. Even with the approximation of these complex signals (for instance, the sum of a number of independent sine waves), the deterministic approach has often proven unacceptable. Usually the number of component signals were inadequate to truly simulate the normal system input. As a result, beat-frequencies or harmonics effects were often missed and the true system performance was not evaluated. To overcome this deficiency, band-limited noise (usually limited to the same operational bandwidth as the tested system) is now often used as a test signal and represents a very general approach to communication system performance evaluation. Yet, while band-limited noise is an excellent tool with which to simulate realistic data conditions, it has proven difficult to uniformly delay — thereby making valid system input/output comparisons difficult to accomplish.

There are two basic ways to test a system utilizing band-limited noise as a test signal — digital and analog (reference Appendix A). With the digital approach, band-limited noise is fed into a test system and the output monitored. The system input is sampled and digitized (thereby the digital notation). These digitized samples are compared with digitized samples of the test system output yielding mean square values of the distortion introduced. Constant gain and average delay factors are compensated so that they do not contribute to the distortion introduced by the system being tested since these

factors are not usually considered as errors. There are two primary advantages of such a scheme: A complex test signal is used that is similar to the expected operational input spectrum, and all operations after sampling are digital. The primary disadvantages are that the effects of system spikes, such as FM "clicks," are often still missed.

In the analog system approach, band-limited noise is fed into a test system. The system output is compared on an rms basis with a delayed and scaled version of the system input. The obvious advantages are that the equipment is compact and relatively simple to build. The largest disadvantage is the difficulty in delaying the complex input without distortion.

The pseudonoise (PN) test set is designed to provide a reliable, operationally simple unit which will allow the previously mentioned analog rms end-to-end error measurement of most communication systems to be easily performed. It also provides a band-limited pseudorandom noise as an input, thereby escaping the disadvantages of most deterministic signals while retaining the advantages of using true band-limited noise. In addition, the PN test set can be used as a means with which the autocorrelation function and impulse response may be determined for certain systems.

II. THEORY OF PSEUDONOISE TESTING

Correctly defined noise signals give a good approximation of the data signals handled by communication systems. The noise signals must be stationary to assure that the measurements are repeatable. Noise can be defined by two unrelated parameters, power spectral density and the amplitude probability density function.

Power spectral density (PSD) describes how the energy in a noise signal is distributed in frequency. Generally, the noise power spectral density, as a function of frequency, can take almost any shape; however, the most common specification is that the power spectral density be constant with frequency. This describes "white" noise.

Probability density function (PDF) of a noise signal is defined as that function which, when integrated over an interval (X_1, X_2), gives the probability that the noise amplitude, X_N, lies in the interval (X_1, X_2). Specifically,

$$P(X_1 \le X_n \le X_2) = \int_{X_1}^{X_2} p(x)\,dx \quad , \tag{1}$$

and $p(x)$ is the amplitude probability density function, PDF.

True noise data signals are difficult to delay without introducing appreciable distortion. This problem is eliminated by using pseudorandom noise signals. PN signals produced by the test set are, in fact, not random but are completely definitive and repetitive. These PN signals can be made to closely resemble true random noise signals from both the power spectral density and probability density function aspects.

A pseudorandom binary sequence can be generated by a shift register with an input dependent on feedback from certain register stages. The maximal length (ML) PN binary sequence is of length L and contains $2^n - 1$ bits before repetition of the sequence (where N is the number of register stages).

An important characteristic of pseudorandom sequences is the correlation property. If a binary sequence is pseudorandom, the correlation function of the sequence, and the sequence shifted with respect to itself, is constant for all shifts other than shifts of an integer number of sequence periods. Specifically, if vector A is a sequence $(a_1, a_2, \ldots, a_n)$, and B is a shifted version of this same sequence (with j shifts), then the correlation function (R) is:

$$R(j) = -\frac{1}{L} \sum_{i=1}^{L} (a_i \oplus b_i) \tag{2}$$

where the $\oplus$ indicates modulo-2 addition. If the sequence is pseudorandom,

$$R(j = 0) = 1 \quad ,$$

$$R(0 < j < N) = 1/L \quad , \tag{3}$$

$$R(j = L) = 1 \text{ where } L = 2^N - 1 \quad .$$

This correlation property of a pseudorandom sequence is particularly important because it verifies that the signal generation approximates a random process.

The power spectrum envelope of a PN sequence is a $(\sin X/X)^2$ curve with the first zero occurring at the sequence clock frequency (ω_k). If the PN sequence is lowpass filtered, with the cutoff frequency (ω_o) restrained to $\omega_o < \omega_k/15$, then the PDF of the resultant analog signal can be approximately Gaussian. However, in section VII a situation is described where the probability density function of the filtered sequence may not be Gaussian.

Noise signals generated by lowpass filtering of ML PN sequences are partially described by the cutoff frequency and order of the filter. The spectrum amplitude is approximately flat for $\omega < \omega_o$, the envelope is down three decibels (dB) at ω_o. At frequencies greater than ω_o, the envelope rolls off at a rate of 6 m dB/octave (where m is the data filter order). The spectrum is not continuous but consists of closely spaced spectral lines $\left[\Delta\omega = \omega_k/\left(2^N - 1\right)\right]$.

Figure 1 is a functional block diagram of the PN test arrangement. The filtered PN sequence is represented as a sum of sinusoids,

$$\sum_{i=1}^{\infty} c_i \cos(\omega_i t) \quad . \tag{4}$$

The filtered sequence is passed through the system with transfer function $H(s)$, and the system output is

$$\sum_{i=1}^{\infty} A_i \cos(\omega_i t + \theta_i) \quad . \tag{5}$$

A scaled and delayed version of the original analog signal is

$$\sum_{i=1}^{\infty} B_i \cos(\omega_i t + \tau\omega_i) \quad . \tag{6}$$
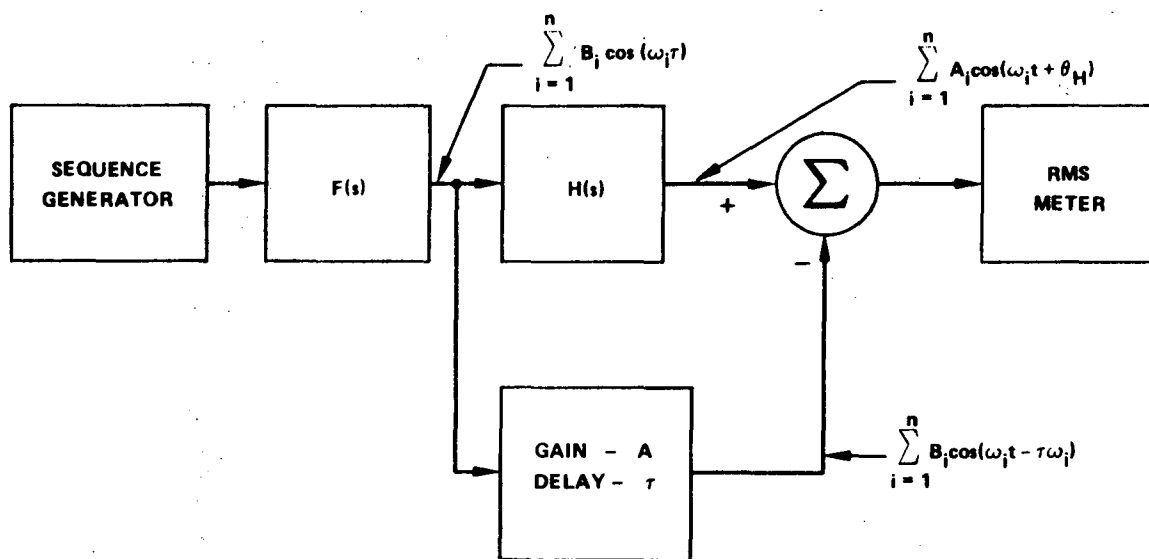
Figure 1. Block diagram of PN test arrangement.

The difference between these two complex waveforms is evaluated on an rms basis by the PN test set to give a figure of merit relating to the system's ability to transfer the complex pseudonoise data signals.

The PN test set was designed to perform the measurement of the waveform distortion as described above. It has been successfully used to measure single-channel and multi-channel performance in CBW/FM communication systems. Specific test procedures were outlined to allow for measurement of the total end-to-end system error as well as the major individual sources of error, namely, channel filter distortion, adjacent channel crosstalk, intermodulation, and RF noise. The measured data have been utilized, in conjunction with analytically derived data, in the analysis of existing telemetry equipment as well as in the designs proposed for new and improved systems.

III. DESCRIPTION OF A PN TEST SET

The PN test set as designed and fabricated provides both real-time and record/playback systems testing capabilities for measuring rms error, system time delay, correlation function, and system impulse response (assuming a linear system).

Components

Basically, the PN test set consists of a pseudorandom binary sequence generator, sequence delay circuitry, spectrum shaping filters, signal conditioning amplifiers, a difference amplifier, a system clock, and tape recorder interface circuitry. Figure 2 is a simplified block diagram of the PN test set. Figure 3 is a photograph of the unit.

Clock. The system clock, a free-running multivibrator is adjusted to provide a 45 kHz output. The clock output consists of a sequence of consecutive binary one's and zero's to the PN sequence generator. The one state is +5.0 Vdc and the zero state is ground level.

PN Sequence Generator. The sequence generator is an ML, 20-stage shift-register with feedback from taps 17 and 20.

Delay Circuitry. There is a delay circuitry (channel) which consists of a NAND gate matrix for coarse delay selection and clock vernier for fine delay control.

Spectrum Shaping Filters. The shaping filters are matched, Butterworth active lowpass filters. Filter insertion loss is zero dB, with zero dB ripple in the response band.

Conditioning Amplifiers. Channels 1 and 2 conditioning amplifiers have gain and dc offset potentiometers (front panel) provided for control of the amplifier outputs.

Difference Amplifier. The difference amplifier consists of three Fairchild 741 operational amplifiers. The amplifiers present a high impedance to the differential inputs, and has a 0.01 ohm output impedance. The difference amplifier has a gain of 2; therefore, the output is 2 times the difference of the 2 inputs.

Recorder Interface. Interface circuits are provided for the record-playback modes of operation. In the record mode, the outputs consist of a differentiated version of the clock and pseudorandom binary sequence. In playback mode, the interface accepts the differentiated signals from the recorder and decodes the clock and binary sequence signals. These signals must have an amplitude of at least 1.3 V at the PN test set input during recorder playback.
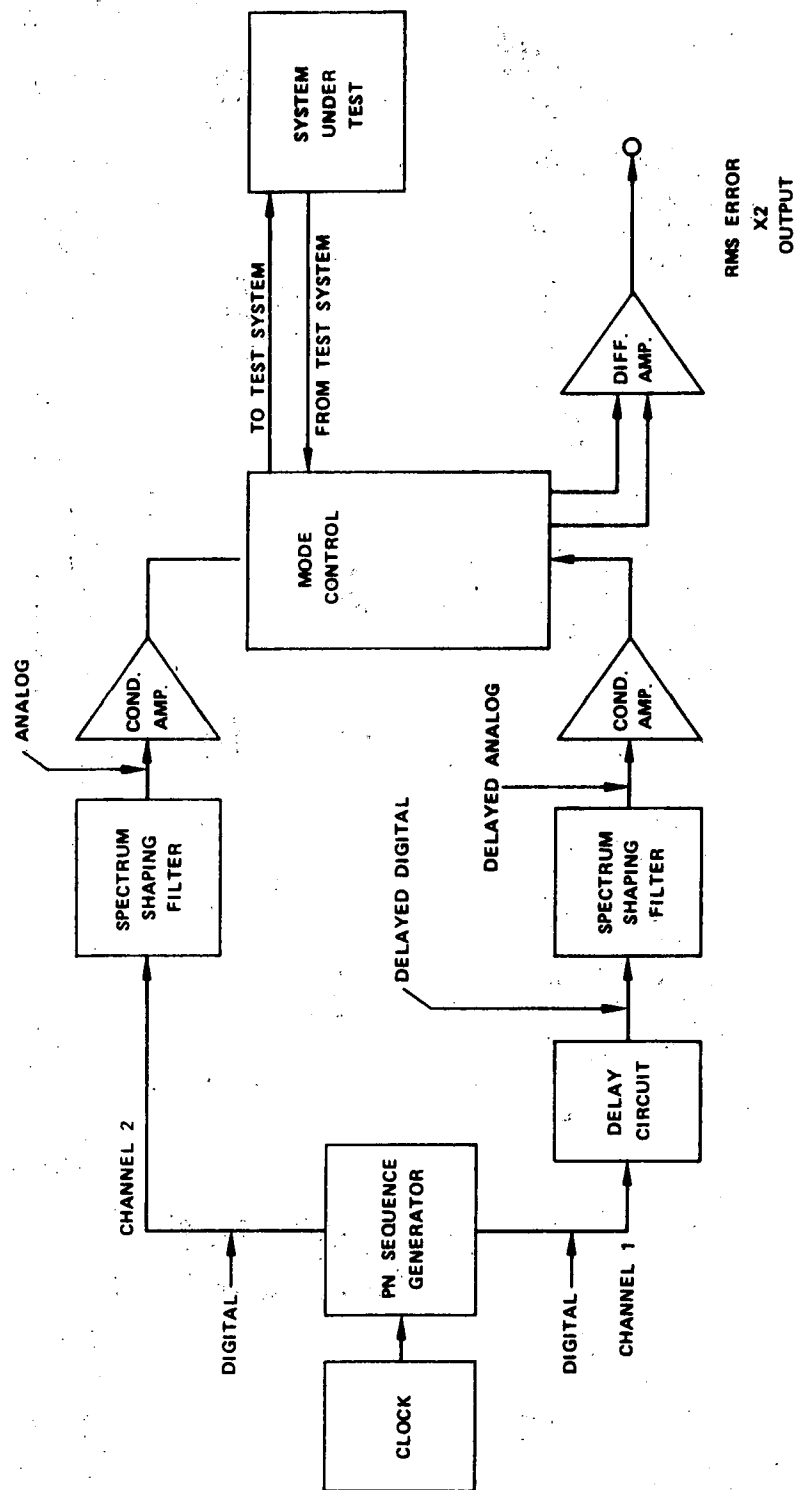
Figure 2. PN test set block diagram.

7
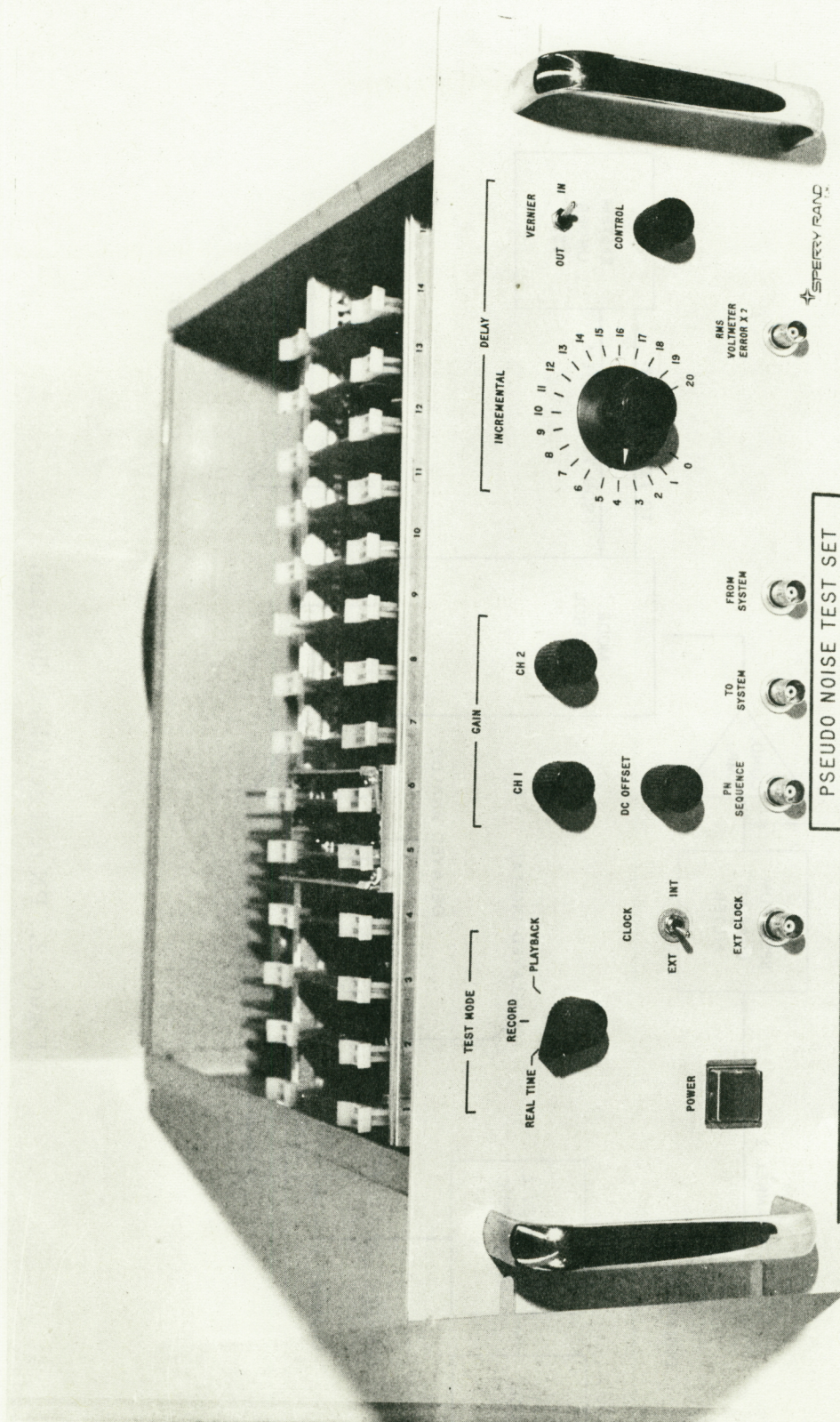
Figure 3. 19 in. rack PN test set.

Electrical Specifications

Inputs

1. Analog response signal from test system.

2. External clock–Internal clock is 45 kHz. If other frequencies are desired, external clocks must be used. The unit has been tested with external clock frequencies up to 1 MHz. However, with the PN sequence generator used to ensure a Gaussian amplitude probability density distribution, the ω_k/ω_o should be 12 to 36 (allowable range).

Outputs

1. Analog signal (filtered PN sequence) to system under test, variable 27 mV (p-p) to 5.5 V (p-p) with adjustable dc offset from –5.0 Vdc to +4.2 Vdc. The power density spectrum envelope of the analog signal is primarily that of the lowpass Butterworth shaping filter (the unit has selectable filter pairs with cutoff frequencies of 400 Hz, 500 Hz 1 kHz, and 2 kHz). The amplitude probability density is near–Gaussian with an adjustable mean.

2. Input/output average delay (back panel) vernier incremental commands to counter and front panel 21 position rotary switch — –11.5 μs to 455 μs, readable to less than 0.1 μs.

3. PN Sequence — from ML PN sequence (20 states) when in record or playback modes (not normal test modes).

4. RMS error output signal — error output from difference amplifier provides interface with true rms (T-rms) voltmeter.

Necessary Auxilliary Equipment. T-rms voltmeter, elapsed time counter (for vernier delay).

Power. 115 Vac, 60 Hz, single phase (less than 3 amps) powers internal 6 Vdc (1.5 A) and ±15 Vdc (0.2 A) power supplies.

IV. DATA FILTERS

Active Data Filters

The pseudonoise test set uses a matched active filter pair, one filter in the output signal channel and one in the reference channel. The filters are matched to minimize the true rms value of the difference in the response functions for a random sequence input. Five interchangeable plug-in filter sets were constructed. Four are Butterworth third-order lowpass filters with 3 dB cutoff frequencies at 400 Hz, 500 Hz, 1000 Hz, and 2000 Hz, and one is a first-order lowpass with 3 dB cutoff at 2000 Hz. The filter order and cutoff frequencies are listed below:

Filter Order (pole)	Cutoff Frequency (Hz)
3	400
3	500
3	1000
3	2000
1	2000

General Design Theory. The filters were synthesized using the active network design procedure given in Computer-Aided Filter Design Manual, section 6.0 [1]. The computer programs provided in the manual were used to design the filters. The filters consist of active second-order (quadratic) lowpass networks. Odd order filters are realized by connecting a first-order lowpass network to the output of the last quadratic network. The quadratic network uses a voltage controlled source type of amplifier having a gain close to unity. In the PN test set, an operational amplifier at unity gain was used. The controlled source type of active network requires the minimum number of circuit components.

The general voltage transfer function of a quadratic lowpass filter is,

$$F(s) = \frac{1}{s^2 + 2\zeta\omega_n s + \omega_n^2} = \frac{\left(\dfrac{1}{\omega_n}\right)^2}{\left(\dfrac{s}{\omega_n}\right)^2 + 2\zeta\left(\dfrac{s}{\omega_n}\right) + 1} \quad . \tag{7}$$

A quadratic (2 pole) lowpass network and a 1 pole lowpass network are connected in cascade to obtain the third-order filter configuration shown in Figure 4. This configuration was used to realize all the third order filters. The variable K is the gain of the amplifier, R_0 is the output resistance of the amplifier, and R_L is the load on the filter.

The normalized transfer function of the quadratic section is

$$\frac{E_2(s)}{E_1(s)} = \frac{Gs^2 + Ds + K}{As^2 + Bs + 1} \tag{8}$$

where

$$A = R_1 R_2 C_1 C_2 \left(1 + \frac{R_0}{R_1} + \frac{R_0}{R_2}\right) , \tag{9}$$

$$B = R_1 C_1 (1 - K) + C_2 (R_1 + R_2) + R_0 C_1 , \tag{10}$$

$$G = R_0 R_2 C_1 C_2 , \tag{11}$$

$$D = R_0 C_1 . \tag{12}$$

Here, R_1 includes the source resistance to the network and C_2 includes the input capacitance of the amplifier.
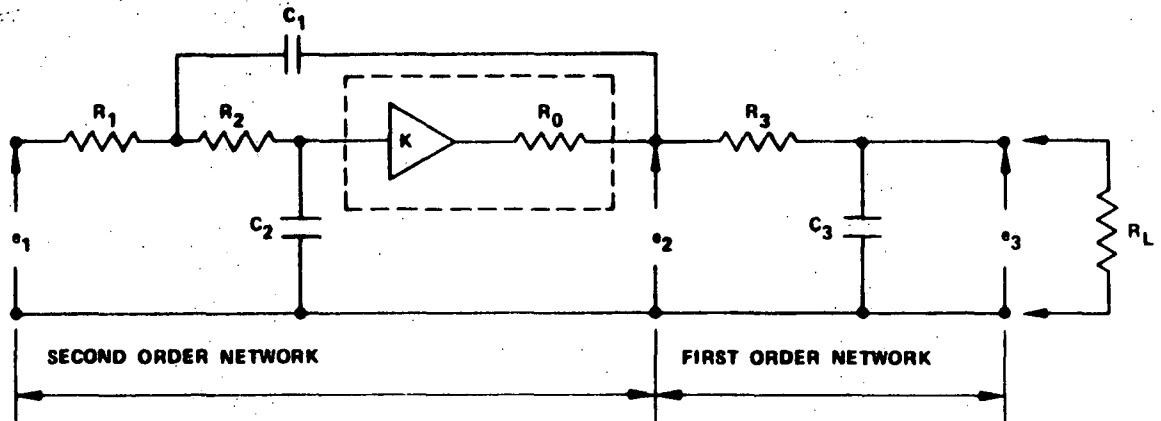
Figure 4. Third-order active lowpass filter.

The normalized transfer function of the first-order section is

$$\frac{E_3(s)}{E_2(s)} = \frac{E}{H\,s\,+\,1} \qquad (13)$$

where

$$E = \frac{R_L}{R_3\,+\,R_L} \quad , \qquad (14)$$

$$H = \frac{R_L\,R_3\,C_3}{R_3\,+\,R_L} \quad . \qquad (15)$$

For the relatively low cutoff frequencies involved and for $K \approx 1$ and $R_0 \approx 0$, the network transfer function of equation (8) reduces to,

$$\frac{E_2(s)}{E_1(s)} = \frac{1}{R_1\,R_2\,C_1\,C_2\,s^2\,+\,C_2\,(R_1\,+\,R_2)\,s\,+\,1} \quad . \qquad (16)$$

The synthesis equations for the networks described by transfer functions (16) and (13) scaled in frequency by ω_0 are

$$R_1 = \frac{1}{\omega_0}\left[\frac{B}{2C_2}\,+\,\sqrt{\left(\frac{B}{2C_2}\right)^2\,-\,\frac{1}{C_1\,C_2}}\;\right], \qquad (17)$$

$$R_2 = \frac{1}{\omega_0}\left[\frac{B}{2C_2}\,-\,\sqrt{\left(\frac{B}{2C_2}\right)^2\,-\,\frac{1}{C_1\,C_2}}\;\right], \qquad (18)$$

$$C_1 \geq \frac{4C_2}{B^2} \quad , \qquad (19)$$

$$R_3 = \frac{1}{\omega_0\,C_3\,-\,\dfrac{1}{R_L}} \qquad (20)$$

12

where ω_o equals the 3 dB cutoff frequency in radians per second, $R_1 R_2 C_1 C_2$ and H are set equal to unity, and $B = C_2 (R_1 + R_2)$. The usual synthesis procedure for the quadratic network is to, first, select a value for C_2 and, then, choose C_1 such that $C_1 \geq 4C_2/B^2$. Then R_1 and R_2 are calculated. For the matched filters, the more accurate synthesis equations of the computer program were used where $K = 0.99999$ and $R_0 = 0.01$ ohms. A thorough development of the exact design equations used is given in a thesis [2] which was the source for much of the active filter material contained in Computer-Aided Filter Design Manual [1].

The normalized pole positions for a third-order Butterworth filter are $s = 0.5000 \pm j0.8600$ and $s = -1.000$. These poles give a lowpass transfer function of

$$F(s) = \frac{1}{s^2 + s + 1} \cdot \frac{1}{s + 1} . \tag{21}$$

To frequency-scale the function to have its 3 dB cutoff at ω_o, the complex operator s is divided by ω_o. The transfer function of equation (21) scaled to have a 3 dB cutoff at ω_o is, therefore,

$$F(s) = \frac{1}{\left(\dfrac{s}{\omega_o}\right)^2 + \left(\dfrac{s}{\omega_o}\right) + 1} \cdot \frac{1}{\left(\dfrac{s}{\omega_o}\right) + 1}$$

$$= \frac{\omega_o^2}{s^2 + \omega_o s + \omega_o^2} \cdot \frac{\omega_o}{s + \omega_o} . \tag{22}$$

Reference to equations (13) and (16) show that coefficients H and B are equal to unity and that the 3 dB cutoff frequency ω_o is equal to the natural frequency ω_n of equation (7).

Matching and Tuning Procedure. An advantage of the active filter design procedure contained in Reference 1 is that tuning can be eliminated or at least held to a minimum. However, because of the extremely close

tolerances required to match the filters to less than 0.1 percent rms error, a rigorous component matching and tuning procedure was necessary. The following procedure is used.

Two sets of approximately matched components are obtained for the values calculated by the computer program. Using one set of components, a filter is breadboarded and slightly tuned, if necessary, to have the specified cutoff frequency. The components are then removed from the breadboard and individually placed on a General Radio Type 1608-A Impedance Bridge. For each component, the bridge meter is nulled. Then, without disturbing the null setting controls, the component is removed and its approximately matched counterpart is placed on the bridge. Without adjusting the bridge controls, the component is then built up or adjusted until the meter reaches the same null. The same procedure is applied to all the components.

A pair of closely matched operational amplifiers is selected from a large group of amplifiers. The amplifier parameters measured for matching purposes are the input capacitance and the output rise time. The filter pair is then constructed using the closely matched component pairs. At this point, the rms error for the third-order, 200-Hz filter was about 0.4 percent. This error is probably due to slight differences in the wiring layout, the amplifier parameters, and the resistive and capacitive components.

To further reduce the rms error requires very fine tuning of the constructed filter pair. Each component of the filter pair is individually tuned while observing the effect on the rms error. First, each resistor is individually paralleled with a 20 to 50 MΩ resistor and the effect noted. If the error is reduced, a parallel resistor is permanently added. Then each capacitor is parallel with a 1 to 3 pF capacitor and the effect is noted. This procedure is repeated several times until minimum rms error is achieved, usually below 0.2 percent. At first the rms error drops only slightly for each component adjustment but begins to drop more rapidly as a more exact filter match is approached. Finally, each resistor is individually paralleled with a capacitor and each capacitor with a resistor, and the effect on the error is noted. This further tuning reduced the rms error of the third-order, 200-Hz filter from 0.1 percent to 0.05 percent.

An advantage of using active filters should be that the second- and first-order sections can be matched separately and then connected. However, this is not the case because of the extremely high degree of matching required. There is still a small amount of interaction between the section which must be

included during the tuning process. When the sections were matched separately and then connected, the combined sections were no better matched than before tuning.

Design Results. The first matched filter set built was a third-order Butterworth with 3 dB cutoff at 2000 Hz. The schematic for this filter pair is shown in Figure 5. The responses of the filter pair are matched to 0.05 percent true rms error. The total set error with the filter plugged in was 0.15 percent. The rest of the prototype test set introduces about 0.1 percent rms error mainly due to radiation of digital switching spikes into the data and differences in output rise times of digital circuits in each channel. This error could be reduced by better separation and shielding of the analog output from the high speed digital circuitry.
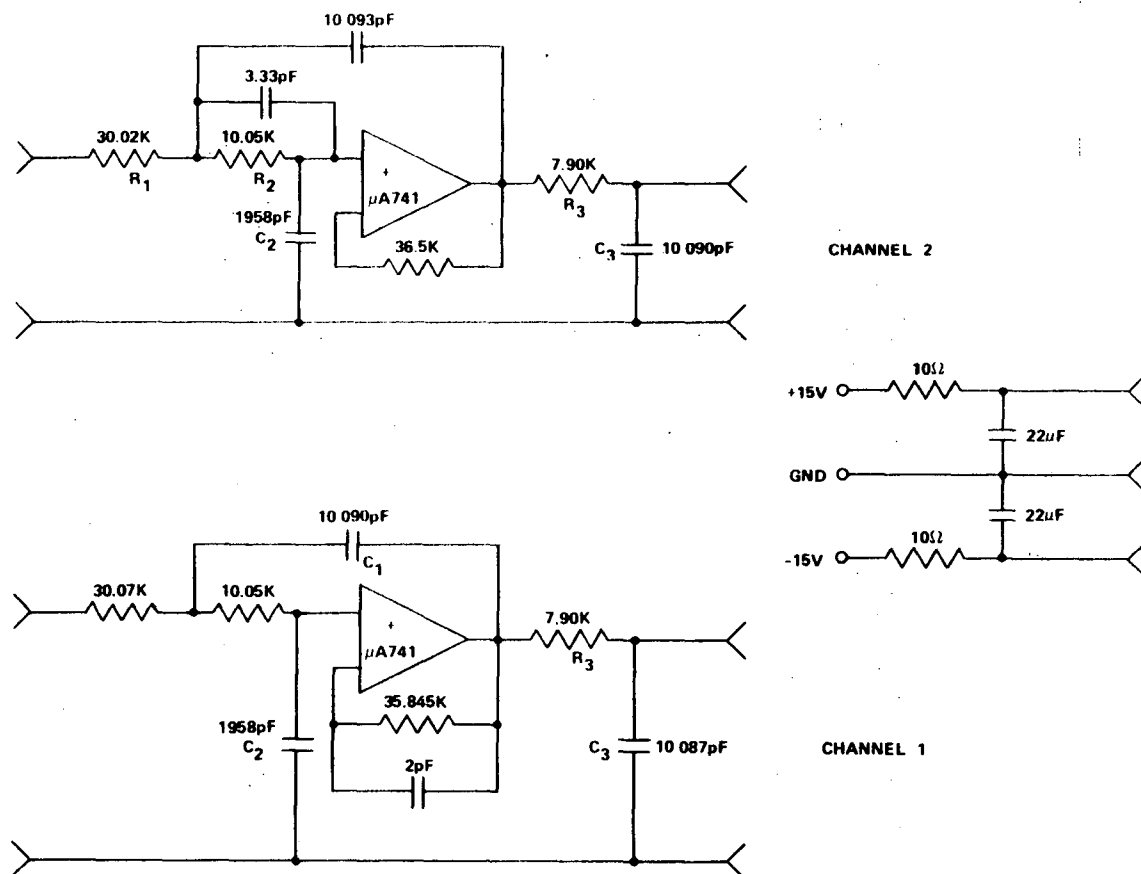

Figure 5. Third-order, 2000-Hz matched filter pair.

Four other filter pairs were constructed having the same configuration as shown in Figure 5. Of course, the one pole filter consisted of only R_3 and C_3. For these four filters, the fine tuning was accomplished by placing trimmer capacitors across all capacitors of one filter pair. By using this procedure, all capacitive tuning could be performed on only one filter as the capacitance could be easily increased or decreased. It was found that it was more difficult to reduce the rms error using the trimmers than with paralleling discrete components.

The component values used for the other four matched filters along with their final rms errors are given below.

For 400 Hz cutoff, third-order filter:

R_1 = 78.596 KΩ C_1 = 23 525 pF

R_2 = 21.552 KΩ C_2 = 3967.8 pF

R_3 = 27.491 KΩ C_3 = 15 448 pF

Filter rms error = 0.12 percent

Total test set error = 0.228 percent (with filter plugged in)

For 500 Hz cutoff, third-order filter:

R_1 = 67.115 KΩ C_1 = 23 394 pF

R_2 = 17.067 KΩ C_2 = 3776 pF

R_3 = 20.9 KΩ C_3 = 15 880 pF

Filter rms error = 0.05 percent

Total test set error = 0.15 percent

For 1 KHz cutoff, third-order filter:

R_1 = 62.377 KΩ C_1 = 11 937 pF

R_2 = 16.959 KΩ C_2 = 2001 pF

R_3 = 20.889 KΩ C_3 = 7997 pF

Total rms error = 0.09 percent

Total test set error = 0.207 percent

For 2000 Hz, first-order filter:

R_3 = 20.054 KΩ C_3 = 3787.2 pF

Filter rms error = 0.08 percent

Total test set error = 0.16 percent

Sensitivity Analysis. Because of the difficult and time-consuming tuning required for construction of the four matched filter pairs, a sensitivity analysis was performed on the active quadratic networks. The damping ratio (ζ) and the natural frequency (ω_n) of the network were taken as being representative parameters of the shape of the response curve. Therefore, the sensitivity of ζ and ω_n were determined for a percentage change in each of the network components. The results indicate that the sensitivity of ζ to changes in R_1 or R_2 is minimum when $R_1 = R_2$, which occurs when $C_2/C_1 = \zeta^2$. The analysis was performed for the simplified case where $K = 1$ and $R_0 = 0$. For designs where $R_0 \neq 0$, R_1 must be somewhat larger than R_2.

Equating the transfer function of the general quadratic function, equation (7), with the quadratic network function, equation (16), where coefficient $B = 2\zeta$ gives ζ and ω_n as

$$\zeta = \sqrt{\frac{C_2}{C_1}} \frac{R_1 + R_2}{2\sqrt{R_1 R_2}} \quad , \tag{23}$$

$$\omega_n = \frac{\omega_L}{\sqrt{R_1 R_2 C_1 C_2}} \quad . \tag{24}$$

where ω_o equals lowpass 3 dB cutoff frequency. Normally $R_1 \cdot R_2 \cdot C_1 \cdot C_2$ is made equal to unity and, therefore, $\omega_n = \omega_o$.

The equations derived for the change in ζ and ω_n for percentage changes in components R_1, R_2, C_1, C_2 and ratio C_2/C_1 are given below. The ratio of C_2/C_1 determines the separation in the values of R_1 and R_2. When $C_2/C_1 = \zeta^2$, $R_1 = R_2$.

$$\frac{\partial \zeta}{\frac{\partial R_L}{R_1}} = \sqrt{\frac{C_2}{C_1}} \frac{R_1 - R_2}{4\sqrt{R_1 R_2}} \tag{25}$$

$$\frac{\partial \zeta}{\frac{\partial R_2}{R_2}} = \sqrt{\frac{C_2}{C_1}} \frac{R_2 - R_1}{4\sqrt{R_1 R_2}} \tag{26}$$

$$\frac{\partial \zeta}{\frac{\partial C_1}{C_1}} = -\frac{\zeta}{2} \tag{27}$$

$$\frac{\partial \zeta}{\frac{\partial C_2}{C_2}} = \frac{\zeta}{2} \tag{28}$$

$$\frac{\partial \zeta}{\frac{\partial \left(\frac{C_2}{C_1}\right)}{\frac{C_2}{C_1}}} = \frac{\zeta}{2} \tag{29}$$

$$\frac{\partial \omega_n}{\frac{\partial R_1}{R_L}} = -\frac{\omega_n}{2} \tag{30}$$

$$\frac{\partial \omega_n}{\frac{\partial R_2}{R_2}} = -\frac{\omega_n}{2} \tag{31}$$

18

$$\frac{\partial \omega_n}{\frac{\partial C_1}{C_1}} = -\frac{\omega_n}{2} \qquad\qquad (32)$$

$$\frac{\partial \omega_n}{\frac{\partial C_2}{C_2}} = -\frac{\omega_n}{2} \qquad\qquad (33)$$

$$\frac{\partial \omega_n}{\frac{\partial \left(\frac{C_2}{C_1}\right)}{\frac{C_2}{C_1}}} = -\frac{\omega_n}{2} \qquad\qquad (34)$$

The previous equations show that the change in ω for a percentage change in R_1 or R_2 is minimum when R_1 equals R_2. The change in ω for a percentage change in either C_1 or C_2 is independent of the component values. However, the change in ζ for an absolute change in C_1 or C_2 is inversely proportional to the value of C_1 or C_2. For example,

$$\frac{\partial \zeta}{\partial C_2} = -\frac{\zeta}{2C_2} \quad .$$

Hence, C_2 should be made as large as possible for ease in making a small change in ζ.

The change in ω_n for a percentage change in any one of the components is independent of any of the components' values. However, the change in ω_n for a change in value of any one component is inversely proportional to that one component. For example,

$$\frac{\partial \omega_n}{\partial R_1} = -\frac{\omega_n}{2R_1} \quad .$$

19

Since the filter is designed by first selecting C_2 and then selecting the ratio $C_1/C_2 \geq 1/\zeta^2$, it appears that the best design for easiest tuning would be to select C_2 as large as possible. Then choose C_1 equal to C_2/ζ^2 which makes R_1 equal R_2. For the four filter pairs constructed, the value of R_1 was much larger than R_2. The tuning might have been somewhat easier if R_1 and R_2 were approximately equal.

Passive Data Filters

The application of passive data filters for the pseudonoise test set has been inhibited because of the difficulty in tuning these type filters. Unlike the active configuration, each filter pole position in a passive filter depends upon the interrelationship of all the network components. This complicates the tuning procedure because the relationship between critical filter network characteristics and the network components can be quite involved. For the purpose of designing passive filters for pseudonoise system testing, an improved filter tuning procedure has been developed. With this procedure, effort in tuning a particular filter element is in proportion to that element's effect upon the critical network parameter. The application of passive data filters for PN testing might be desirable if the tuning procedure developed for the passive design results in a very accurately tuned filter.

The tuning procedure developed uses the rms value of the difference in the response functions of a filter and its theoretical perfect reference as the critical parameter. This rms difference is calculated as a function of the variation of each filter element from its synthesized value. Assuming that the rms difference function is accepted as the critical parameter in filter design, then those elements whose variation most affect this parameter should receive proportionally more effort to assure their accuracy.

Mathematical Model. Figure 6 is a block diagram of the basic model. The uniform spectral generator drives each filter with a waveform that has a constant power spectral density. Each filter weights and delays the spectral components, and the normalized rms value of the difference waveform is the critical parameter.
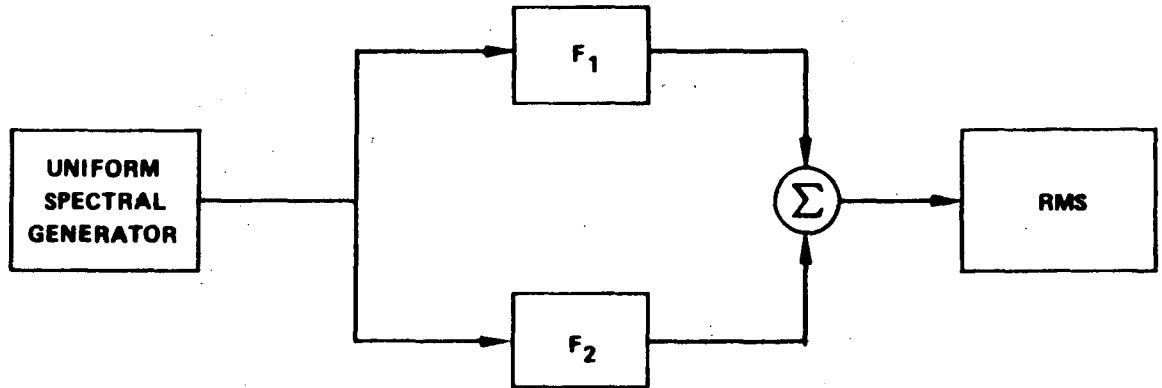
Figure 6. Basic model block diagram.

The normalized mean-square error can be expressed as

$$\frac{\sigma^2}{\sigma_0^2} = \frac{\overline{\int_{-\infty}^{\infty} \{F_1(\omega) \mid \cos[\omega t - \theta_1(\omega)] - \mid F_2(\omega) \mid \cos[\omega t - \theta_2(\omega)]\}^2 d\omega}}{\int_{-\infty}^{\infty} \overline{\mid F_1(\omega) \mid^2 \cos^2[\omega t + \theta_1(\omega)] d\omega}}$$

(35)

In expression (35), the over-bar indicates time average, and other terms are defined as follows:

$F_1(\omega)$ transfer function of the first (reference) filter.

$F_2(\omega)$ transfer function of the second (modified) filter.

Define:

$$F_1(\omega) = \frac{1}{D_1(\omega)} = \frac{1}{Re[D_1(\omega)] + jIm[D_1(\omega)]} = \mid F_1(\omega) \mid \epsilon^{j\theta_1(\omega)} \quad (36)$$

$$F_2(\omega) = \frac{1}{D_2(\omega)} = \frac{1}{\mathrm{Re}[D_2(\omega)] + j\mathrm{Im}[D_2(\omega)]} = |F_2(\omega)| e^{j\theta_2(\omega)} \qquad (37)$$

where

$$\theta_1(\omega) = -\tan^{-1}\left\{\frac{\mathrm{Im}[D_1(\omega)]}{\mathrm{Re}[D_1(\omega)]}\right\} \quad , \qquad (38)$$

$$\theta_2(\omega) = -\tan^{-1}\left\{\frac{\mathrm{Im}[D_2(\omega)]}{\mathrm{Re}[D_2(\omega)]}\right\} \quad , \qquad (39)$$

and $D_1(\omega)$ and $D_2(\omega)$ are complex polynomials in ω. Expanding the expression taking the time average yields

$$\frac{\sigma^2}{\sigma_0^2} = \left\{\int_{-\infty}^{\infty} |F_1(\omega)|^2\, d\omega - 2\int_{-\infty}^{\infty} |F_1(\omega)|\, |F_2(\omega)|\, \cos[\theta_1(\omega) - \theta_2(\omega)]\, d\omega \right.$$
$$\left. + \int_{-\infty}^{\infty} |F_2(\omega)|^2\, d\omega \right\} \bigg/ \left[\int_{-\infty}^{\infty} |F_1(\omega)|^2\, d\omega\right] \quad , \qquad (40)$$

or

$$\frac{\sigma^2}{\sigma_0^2} = \left\{\int_{-\infty}^{\infty} |F_1(\omega)|^2\, d\omega - 2\int_{-\infty}^{\infty} |F_1(\omega)|\, |F_2(\omega)|\, \cos[\theta_1(\omega)]\, \cos[\theta_2(\omega)]\, d\omega \right.$$

$$- 2\int_{-\infty}^{\infty} |F_1(\omega)|\, |F_2(\omega)|\, \sin[\theta_1(\omega)]\, \sin[\theta_2(\omega)]\, d\omega$$

$$\left. + \int_{-\infty}^{\infty} |F_2(\omega)|^2\, d\omega \right\} \bigg/ \left[\int_{-\infty}^{\infty} |F_1(\omega)|^2\, d\omega\right] \quad , \qquad (41)$$

Substituting into equation (41), the relations

$$\cos[\theta_1(\omega)] = \text{Re}[D_1(\omega)] \ |F_1(\omega)| \quad , \tag{42}$$

$$\sin[\theta_1(\omega)] = -\text{Im}[D_1(\omega)] \ |F_1(\omega)| \quad , \tag{43}$$

$$\cos[\theta_2(\omega)] = \text{Re}[D_2(\omega)] \ |F_2(\omega)| \quad , \tag{44}$$

$$\sin[\theta_2(\omega)] = \text{Im}[D_2(\omega)] \ |F_2(\omega)| \tag{45}$$

yield

$$\frac{\sigma^2}{\sigma_0^2} = \left\{ \int_{-\infty}^{\infty} |F_1(\omega)|^2 \, d\omega - 2 \int_{-\infty}^{\infty} |F_1(\omega)|^2 |F_2(\omega)|^2 \, \text{Re}[D_1(\omega)] \, \text{Re}[D_2(\omega)] \, d\omega \right.$$

$$- 2 \int_{-\infty}^{\infty} |F_1(\omega)|^2 \, |F_2(\omega)| \, \text{Im}[D_1(\omega)] \cdot \text{Im}[D_2(\omega)] \, d\omega$$

$$\left. + \int_{-\infty}^{\infty} |F_2(\omega)|^2 \, d\omega \right\} \Big/ \left[\int_{-\infty}^{\infty} |F_1(\omega)|^2 \, d\omega \right]$$

$$= (I_2 - 2I_3 - 2I_4 + I_2)/I_1 \quad . \tag{46}$$

Equation (46) may be used to perform an element sensitivity analysis for networks whose transfer functions can be expressed as

$$F(w) = \frac{1}{D(w)} \tag{47}$$

where w is some function of ω. The use of w allows the analysis of bandpass, lowpass, and band-stop filter configurations by transforming to a lowpass equivalent form, equation (47).

<u>Filter Specialized to Cauer Configurations.</u> Figure 7 contains block diagrams of the Cauer singly terminated networks for odd and even orders respectively. Figure 8 shows a section of the ladder network where the elements have been specialized to a lowpass configuration.

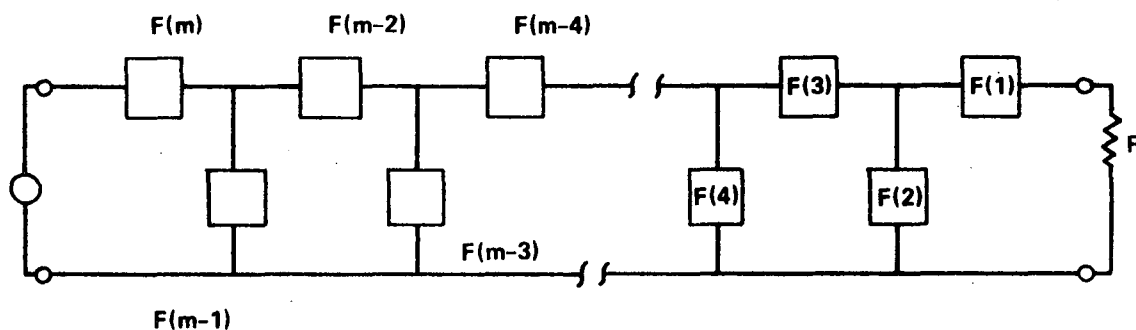The dissipative and reactive components in each element may be lumped together by defining

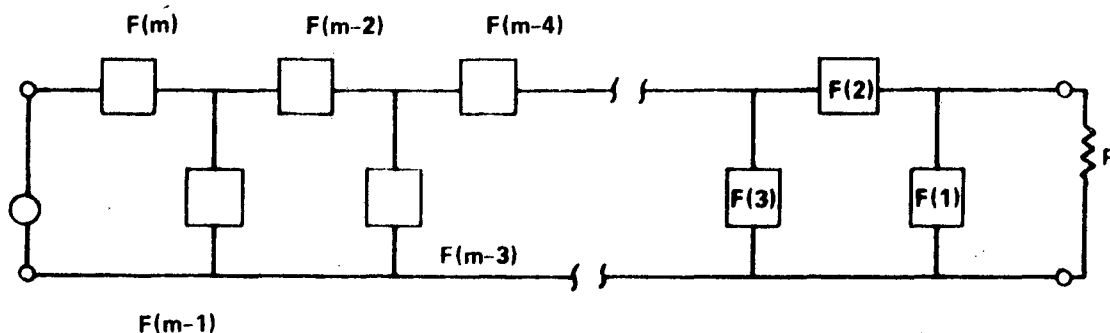$$j\omega^* = j\omega + d \qquad\qquad\qquad (48)$$

where

$$d = 1/Q \quad , \qquad\qquad\qquad (49)$$

and d is called the element dissipation factor, Q is the element quality factor, and ω^* is called the dissipative frequency term.

a. Odd order.

b. Even order.

Figure 7. Cauer configuration.
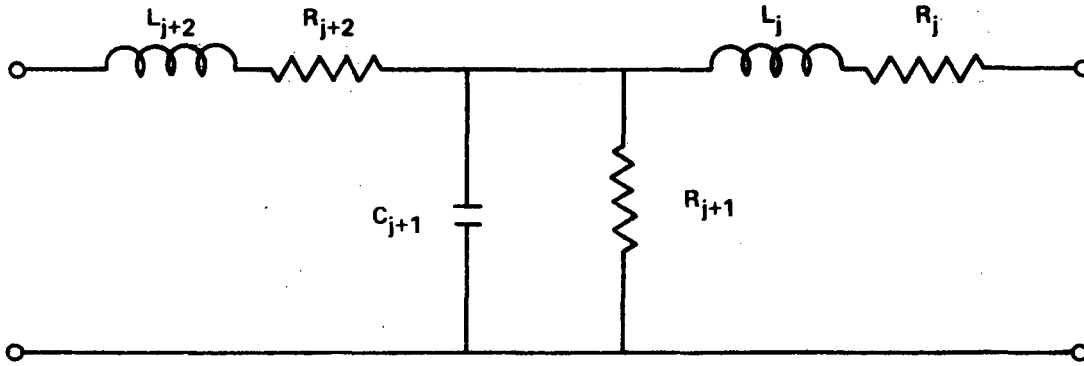
Figure 8. Section of a ladder network, specialized
to a lowpass configuration.

Realization of Chebyshev and Butterworth Filters. The form of the
Butterworth transfer function is

$$F(\omega) = \frac{1}{\sqrt{1 + \omega^{3N}}} \tag{50}$$

where N is the filter order. The form of the Chebyshev transfer function is

$$F(\omega) = \frac{1}{\sqrt{1 + \epsilon^2 T_N^2 (\omega)}} \tag{51}$$

where ϵ is a real constant, $\epsilon < 1$, and $T_N (\omega)$ is the nth order Chebyshev
polynomial defined as

$$T_N(\omega) = \cos (n \cos^{-1} Z) \tag{52}$$

where Z is a real variable, $Z \leq 1$.

Reference 1 lists a group of programs that synthesize filter elements for Chebyshev and Butterworth filters. These programs perform the following functions:

     1.   Using an expansion of the Chebyshev polynomial calculate the poles of $F(\omega)$.

     2.   Predistort the pole plot to accommodate dissipative components in the filter elements.

     3.   Perform a synthetic division to calculate ladder (Cauer configuration) element values.

The actual synthesis procedure involves the following steps:

The transfer emittance of a terminated ladder network is

$$\frac{I_2}{V_1} = -Y_{12} = \frac{Y_{12}\, G_2}{G_2 + Y_{22}} \tag{53}$$

where G_2 is the admittance of the termination. If G_2 is normalized to 1, this equation takes the form

$$-Y_{12} = \frac{-Y_{12}}{1 + Y_{22}} \quad . \tag{54}$$

The transfer function of the network is

$$G_{12} = \frac{-Y_{12}}{G_2 + Y_{22}} \quad , \tag{55}$$

and in the case of normalized load impedance, it is seen that

$$G_{12} = \frac{-Y_{12}}{1 + Y_{22}} \quad . \tag{56}$$

The transfer function can be written in the form

$$G_{12} = \frac{P(s)}{q_1(s) + q_2(s)} \qquad (57)$$

where $q_1(s)$ is a polynomial composed of the even powers of the polynomial in the denominator of the transfer function, and $q_2(s)$ is the polynomial composed of the odd powers. Also, equation (57) can be rewritten as

$$-Y_{12} = \frac{P(s)}{q_1(s) + q_2(s)} = \frac{\dfrac{P(s)}{q(s)}}{1 + \dfrac{q_2(s)}{q_1(s)}} \qquad (58)$$

and

$$Y_{22} = \frac{q_2(s)}{q_1(s)} . \qquad (59)$$

If the choice of $q_1(s)$ and $q_2(s)$ was not made in the manner given, the network would not be realizable as a grounded structure.

Figure 9 is a block diagram of the transfer function calculation and filter element modification portion of the program. The first block represents the transfer function calculation from the Chebyshev polynomial expansion. The second block includes the isolation of the output admittance Y_{22} by assuming a normalized resistive termination.

The parallel paths include the calculation of the transfer function for both the reference filter and the modified filter. This procedure may appear redundant because the transfer function for the reference filter is available in block number 1 of Figure 9. The procedure given was selected to minimize the effect of round-off error in the numerical calculations.

The transfer functions are calculated from the modified and unmodified network elements by solving a matrix equation of the form
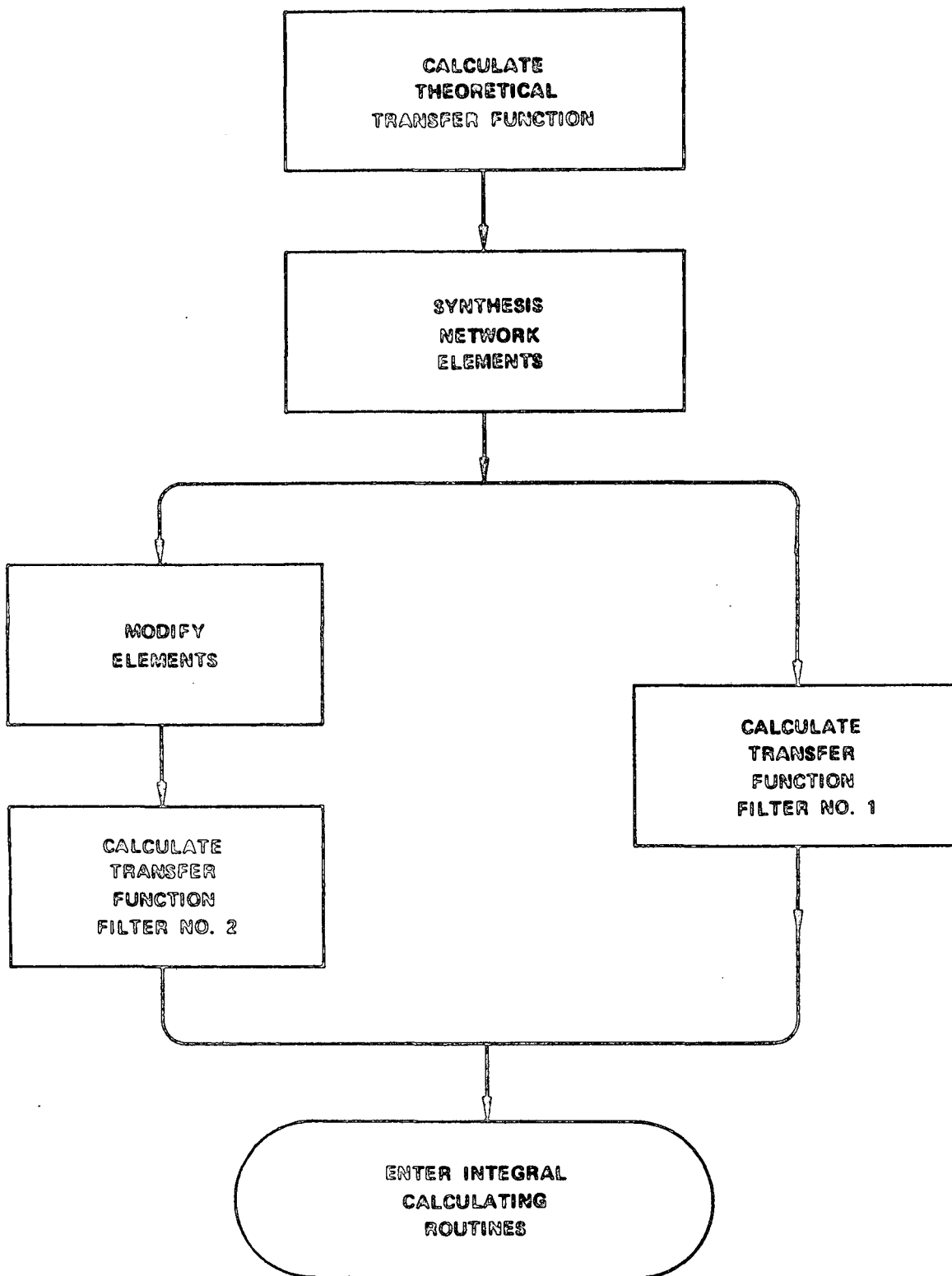
$$KI = E \qquad (60)$$

Figure 9.   Transfer function calculation and filter element
modification block diagram.

where

$$
I = \begin{cases} \left(\dfrac{m}{2} + 1 \right) \text{ order vector, m even} \\[2ex] \left(\dfrac{m+1}{2} \right) \text{ order vector, m odd} \end{cases} ,
$$

$$
E = \begin{cases} \left(\dfrac{m}{2} + 1 \right) \text{ order vector, m even} \\[2ex] \left(\dfrac{m+1}{2} \right) \text{ order vector, m odd} \end{cases}
$$

where $E_1 \neq 0$, $E_i = 0$, $i \neq 1$,

$$
K = \begin{cases} \left(\dfrac{m}{2} + 1 \right) \text{ order matrix, m even} \\[2ex] \left(\dfrac{m+1}{2} \right) \text{ order matrix, m odd} \end{cases} .
$$

The K matrix is symmetrical about the diagonal, $K^T = K$, and $k_{ij} = 0$, $j - 1 > i > j + 1$, where k_{ij} is the ijth element of the K matrix.

Example for a First-Order Filter. A first-order filter in the configuration synthesized by the method of Reference 2 is shown in Figure 10.

The dissipative frequency term

$$
\omega^* = \omega - jd
$$
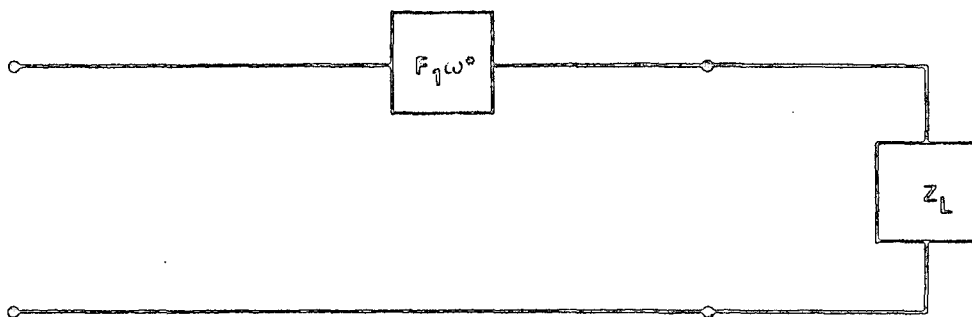
Figure 10. Cauer configuration for a first-order filter.

was defined in equation (48). As an example of the type of calculations performed by the sensitivity programs, a first-order example is given here. The transfer function of the filter is

$$G_{12} = \cfrac{1}{\cfrac{F_1}{Z_L}(j\omega) + \left(\cfrac{F_N \, d_1 + Z_L}{Z_L}\right)} \qquad (61)$$

where d_1 is the dissipative component of the network element, and F_1 is the reactive component.

To simplify the calculations for illustrative purposes, assume for the reference filter in Figure 10 $F_1 = 1$, $Z_L = 1$, and $d_1 = 0$.

From Reference 3,

$$a_{1,1} = \frac{F_1}{Z_L} = 1 \quad , \qquad (62)$$

$$a_{1,2} = \frac{F_1 \, d_1 + Z_L}{Z_L} = 1 \quad , \qquad (63)$$

$$a_{2,1} = \frac{\overline{F}_1}{\overline{Z}_L} \quad , \tag{64}$$

$$a_{2,2} = \frac{\overline{F}_1 \overline{d}_1 + \overline{Z}_1}{\overline{Z}_1} \quad . \tag{65}$$

The terms with bars indicate parameters from the F_2 filter in Figure 10. Referring to equation (46), the integrals can be evaluated as follows.

Evaluation of I_1:

$$D_1 = a_{1,2} = 1$$

$$D_2 = a_{1,2} = 1$$

$$g_1 = 1$$

$$I_1 = (g_1/2D_1 D_2) = 1/2 \quad . \tag{66}$$

Evaluation of I_2:

$$D_1 = a_{2,2} = \frac{\overline{F}_1 \overline{d}_1 + \overline{Z}_L}{\overline{Z}_L}$$

$$D_2 = a_{2,1} = \frac{\overline{F}_1}{\overline{Z}_L}$$

$$g_1 = 1$$

$$I_2 = \frac{g_1}{2D_1 D_2} = \frac{\left(\overline{Z}_L\right)^2}{2\overline{F}_1 \left(\overline{F}_1 \overline{d}_1 + \overline{Z}_L\right)} \quad . \tag{67}$$

Evaluation of I_3:

$$D_1 = a_{1,2} \, a_{2,2} = \frac{\overline{F}_1 \, \overline{d}_1 \, + \, \overline{Z}_L}{\overline{Z}_L}$$

$$D_2 = a_{1,2} \, a_{2,1} + a_{1,1} \, a_{2,2} = \frac{\overline{F}_1}{\overline{Z}_L} + \frac{\overline{F}_1 \, \overline{d}_1 \, + \, \overline{Z}_L}{\overline{Z}_L}$$

$$D_3 = a_{1,1} \, a_{2,1} = \frac{\overline{F}_1}{\overline{Z}_L}$$

$$g_1 = 0$$

$$g_2 = a_{1,2} \, a_{2,2} = \frac{\overline{F}_1 \, \overline{d}_1 \, + \, \overline{Z}_L}{\overline{Z}_L}$$

$$I_3 = \frac{-\, g_1 \, D_1 \, + \, g_2 \, D_3}{2 D_1 \, D_2 \, D_3} \cdot \frac{\overline{Z}_L}{2\left(\overline{F}_1 \, + \, \overline{F}_1 \, \overline{d}_1 \, + \, \overline{Z}_L\right)} \qquad (68)$$

Evaluation of I_4:

$$D_1 = a_{1,2} \, a_{2,2} = \frac{\overline{F}_1 \, \overline{d}_1 \, + \, \overline{Z}_L}{\overline{Z}_L}$$

$$D_2 = a_{1,2} \, a_{2,1} + a_{1,1} \, a_{2,2} = \frac{\overline{F}_1}{\overline{Z}_L} + \frac{\overline{F}_1 \, \overline{d}_1 \, + \, \overline{Z}_L}{\overline{Z}_L}$$

$$D_3 = a_{1,1} \, a_{2,1} = \frac{\overline{F}_1}{\overline{Z}_L}$$

$$g_1 = - a_{1,1} a_{2,1} = \frac{\overline{F}_1}{\overline{Z}_L}$$

$$g_2 = 0$$

$$I_4 = \frac{- g_1 D_1 + g_2 D_3}{2 D_1 D_2 D_3} = \frac{\overline{Z}_L}{2 \left(\overline{F}_1 + \overline{F}_1 \overline{d}_1 + \overline{Z}_L \right)} \qquad . \qquad (69)$$

From equation (69), the normalized mean square error is

$$\epsilon = 1 - \frac{4 \overline{Z}_L}{\overline{F}_1 + \overline{F}_1 \overline{d}_1 + \overline{Z}_L} + \frac{Z_L^2}{(\overline{F}_1) \left(\overline{F}_1 \overline{d}_1 + \overline{Z}_L \right)} \qquad , \qquad (70)$$

where ϵ is equal to σ^2 / σ_0^2. As a check of equation (70) note that if $\overline{Z}_L = 1$, $\overline{F}_1 = 1$, and $\overline{d}_1 = 0$, then $\epsilon = 0$. This is a perfect match with the reference filter.

The three parameters that can vary in the first-order filter are the following:

1. $\overline{d}_1$, the dissipative component.

2. $\overline{Z}_L$, the terminal impedance.

3. $\overline{F}_1$, the reactive component.

Case 1: $\overline{Z}_1 \neq 1$, $\overline{F}_1 = 1$, $\overline{d}_1 = 0$

$$\epsilon = 1 - \frac{4 \overline{Z}_L}{1 + \overline{Z}_L} + \overline{Z}_L \qquad (71)$$

The dependance of ϵ upon $\overline{Z}_L$ for Case 1 is illustrated in Figure 11.

33
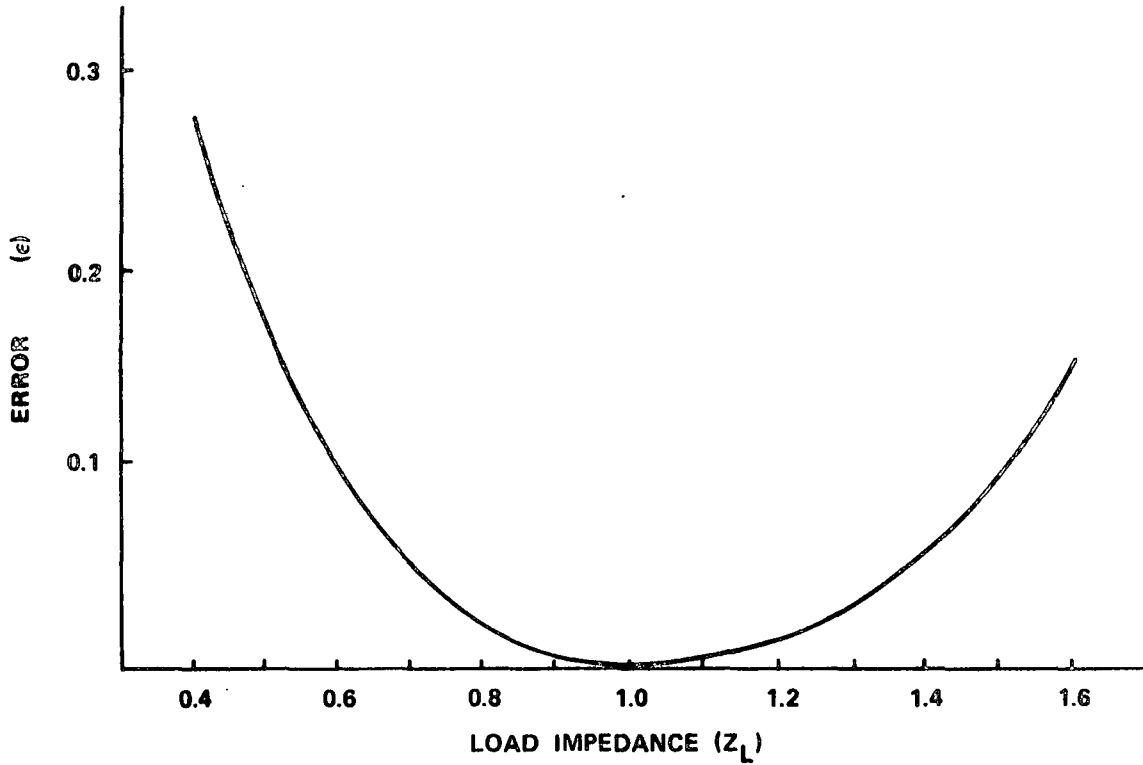
Figure 11. ϵ as a function of $\overline{Z}_L$.

Case 2: $\overline{F}_1 \neq 1$, $\overline{Z}_1 = 1$, $\overline{d}_1 = 0$

$$\epsilon = 1 - \frac{4}{\overline{F}_1 + 1} \cdot \frac{1}{\overline{F}_1} \qquad (72)$$

The dependance of ϵ upon $\overline{F}_1$ for Case 2 is illustrated in Figure 12.

Case 3: $\overline{d}_1 \neq 0$, $\overline{F}_1 = 1$, $\overline{Z}_L = 1$

$$\epsilon = 1 - \frac{4}{2 + \overline{d}_1} + \frac{1}{1 + \overline{d}_1} \qquad (73)$$

The dependance of ϵ upon $\overline{d}_1$ for Case 3 is illustrated in Figure 13.
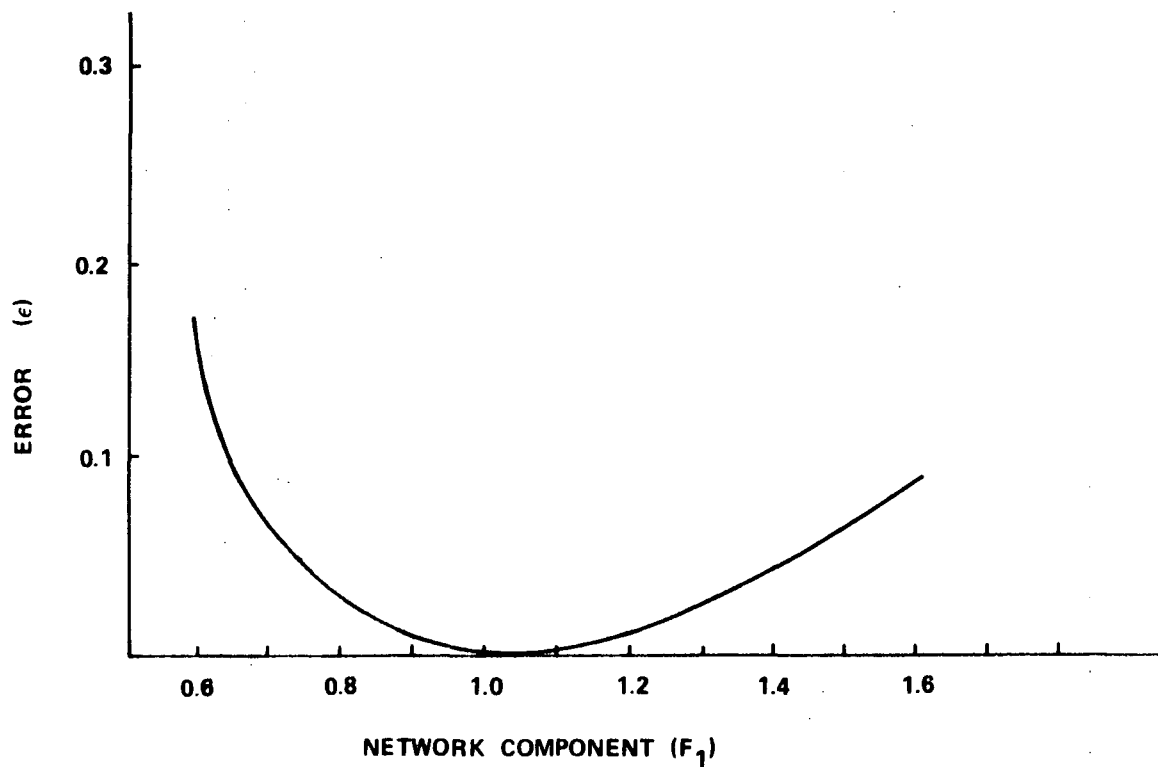
Figure 12. ϵ as a function of $\overline{F}_1$.
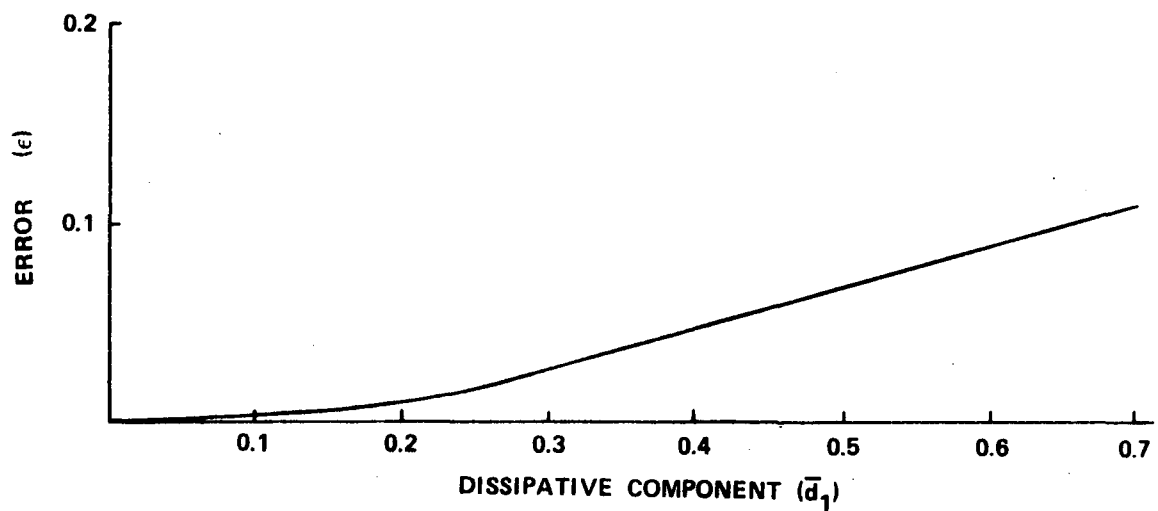

Figure 13. ϵ as a function of $\overline{d}_1$.

The variations of ϵ for the three cases given include a wide range of variations of the network elements. Normally, relatively close adjustment of each parameter can be achieved with a reasonable tuning procedure. More useful information in this case would be a parameter reflecting the sensitivity of ϵ to each parameter near its specified value. A useful parameter for this purpose is the partial derivative of ϵ with respect to the network element of interest. For the first-order filter, these include:

$$\frac{\partial \epsilon}{\partial \overline{Z}_L} \bigg|_{\substack{\overline{d}_1 = 0 \\ \overline{F}_1 = 1}} = \frac{\left(\overline{Z}_L + 3\right)\left(\overline{Z}_L - 1\right)}{\left(\overline{Z}_L + 1\right)^2} \, , \tag{74}$$

$$\frac{\partial \epsilon}{\partial \overline{F}_1} \bigg|_{\substack{d_1 = 0 \\ Z = 1}} = \frac{(3\overline{F}_1 + 1)(\overline{F}_1 - 1)}{\overline{F}_1^2 (\overline{F}_1 + 1)^2} \tag{75}$$

$$\frac{\partial \epsilon}{\partial \overline{d}_1} \bigg|_{\substack{F_1 = 1 \\ Z = 1}} = \frac{\overline{d}_1 (3\overline{d}_1 + 4)}{(\overline{d}_1 + 2)^2 (\overline{d}_1 + 1)^2} \, . \tag{76}$$

If the values of the network parameters are near their design value, $\overline{F}_1 = 1 + \Delta \overline{F}_1$, $\overline{d}_1 = \Delta \overline{d}_1$, and $\overline{Z} = 1 + \overline{Z}_L$ for the example given, then

$$\frac{\partial \epsilon}{\partial \overline{Z}_L} \bigg|_{\substack{\overline{d}_1 = 0 \\ \overline{F}_1 = 1}} \approx \frac{\Delta \overline{Z}_L}{1 + \Delta \overline{Z}_L} \, , \tag{77}$$

$$\frac{\partial \epsilon}{\partial \overline{F}_1} \bigg|_{\substack{\overline{d}_1 = 0 \\ \overline{Z}_L = 1}} \approx \frac{\Delta \overline{F}_1}{1 + 3\Delta \overline{F}_1} \, , \tag{78}$$

$$\frac{\partial \epsilon}{\partial \overline{d}} \bigg|_{\substack{\overline{F}_1 = 1 \\ \overline{Z}_L = 1}} \approx \frac{\Delta \overline{d}_1}{1 + 3\Delta \overline{d}_1} \, , \tag{79}$$

where $\Delta \overline{Z}$, $\Delta \overline{F}_1$, and $\Delta \overline{d}_1$ are small.

The tuning procedure developed should improve the performance of passive filters for applications where accurately matched transfer functions are required. The transfer function match requirements upon the data filters in pseudonoise system testing should be within the capabilities of passive filters if this tuning procedure is applied to the filter manufacture.

V. PREPARATION AND OPERATION OF PN TEST SET

Preparation

This section discusses the PN test set installation, controls, and indicators.

Installation. The PN test set chassis was designed for mounting in a standard equipment rack. A power cable is provided for connection to a 115/125 Vac power source. All system interconnects are on the front panel. Two BNC connectors are mounted on the back panel to facilitate use of an electronic counter to measure exact vernier delay.

Controls and Indicators. Controls and indicators on the PN test set front panel (Fig. 14) are shown in Table 1.

Operation

This section describes normal use of the PN test set to evaluate characteristics of a telemetry-communication system in both the real-time and record-playback modes of operation.

Real-Time rms Error Measurement.

Measurement. Measurement of real-time rms error due to waveform distortion in a communication system can be accomplished by the following procedure.

1. Connect the test setup as shown in Figure 15.

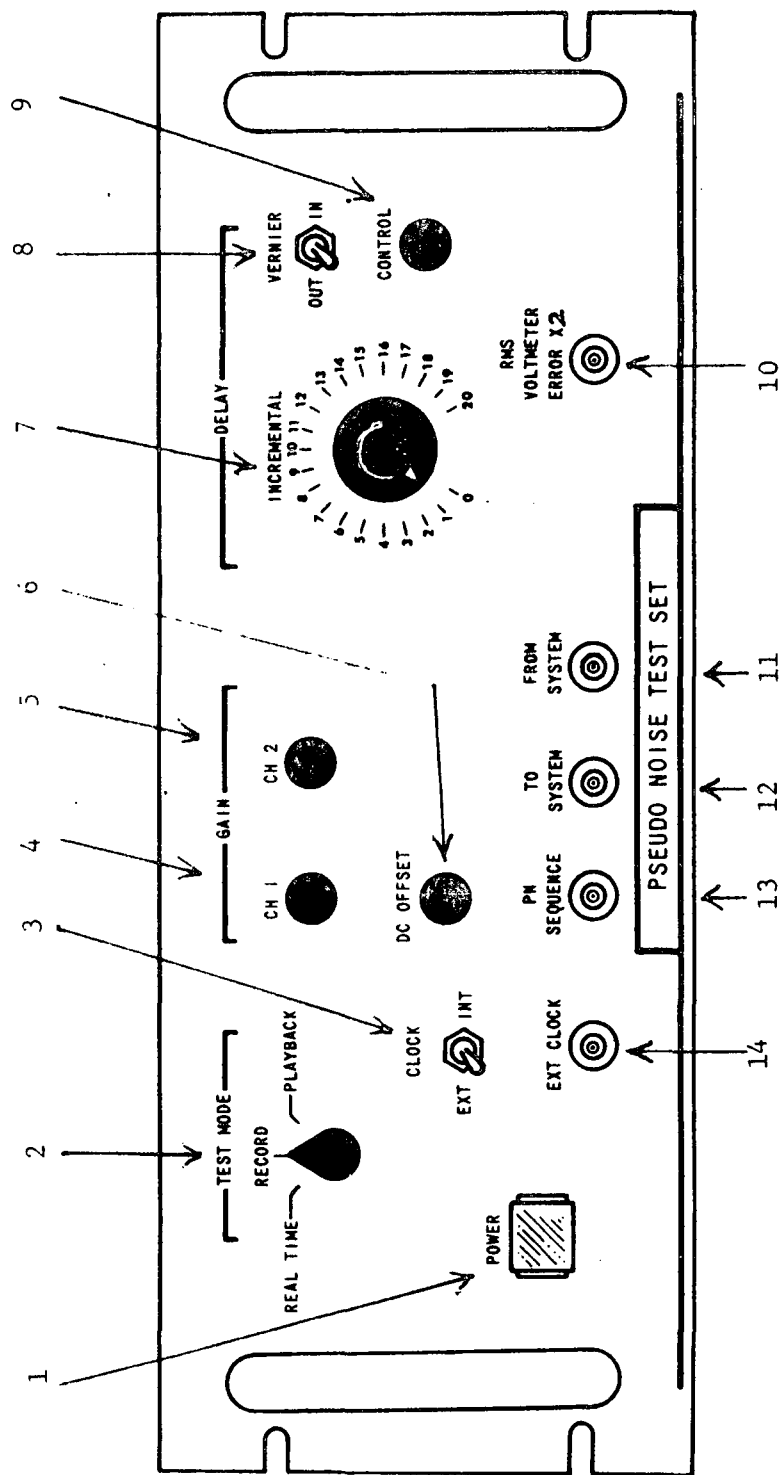2. Place the test set mode switch in the real time position.

Figure 14. PN test set controls.

TABLE 1. PN TEST SET CONTROLS

Key	Control	Type	Purpose
1	POWER	Pushbutton switch	Applies 115/125 Vac power to the test set
2	TEST MODE	3-position rotary switch	Selects mode of operation
3	CLOCK	Two-position toggle switch	Selects internal or external clock
4	GAIN CH 1	10-turn potenti-ometer	Controls gain of the reference signal during REAL TIME and PLAYBACK operation; Controls gain of data signal during RECORD operation
5	GAIN CH 2	10-turn potenti-ometer	Controls gain of the data signal during REAL TIME operation
6	DC OFFSET	1-turn potentiom-eter	Not used, control is now on card 6
7	DELAY INCRE-MENTAL	21-position rotary switch	Selects CH 1 delay in 22.2 μs steps
8	DELAY VERNIER IN-OUT	2-position toggle	Switches VERNIER DELAY circuit into total delay circuit
9	DELAY CONTROL	1-turn potentiom-eter	Controls CH 1 vernier delay from $-11.1\,\mu$s to $+11.1\,\mu$s
10	RMS VOLTMETER ERROR X2	BNC Connector	Provides connection to an rms voltmeter for meas-urement of X2 error

TABLE 1. (Concluded)

| Key	Control	Type	Purpose
11	FROM SYSTEM	BNC Connector	Input from system under test during REAL TIME and PLAYBACK operation
12	TO SYSTEM	BNC Connector	Data output to system under test during REAL TIME and RECORD operation
13	PN SEQUENCE	BNC Connector	Output/input for PN recording track during RECORD and PLAYBACK operation
14	EXT CLOCK	BNC Connector	Output jack for clock signal recording during RECORD and clock input during PLAYBACK
Back Panel Controls			
	EXT CLOCK	BNC	Input jack for external clock during REAL time and RECORD
	START DELAY	BNC	Output jack for reference clock
	STOP DELAY	BNC	Output jack for delayed clock
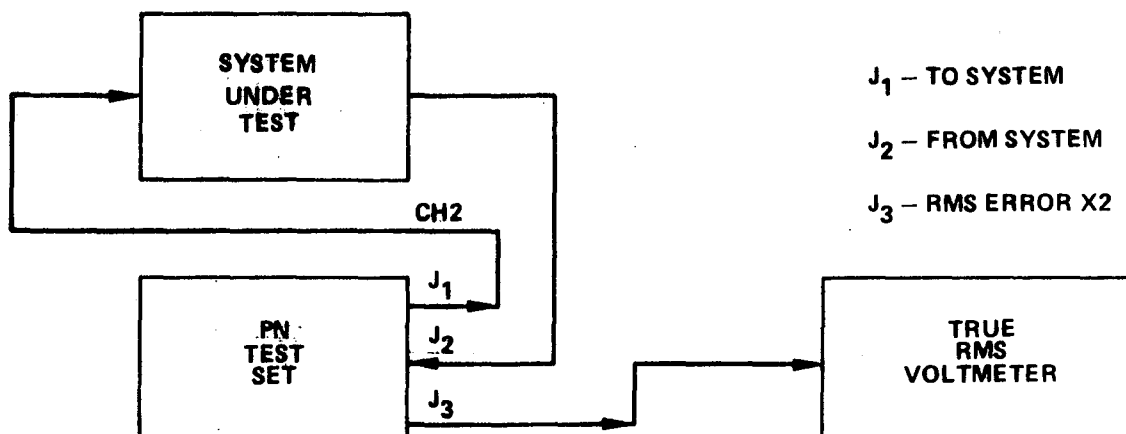
Figure 15. Test setup for real-time rms error measurement.

3. Adjust channel 2 gain control to the correct system dynamic range.

4. Adjust the front panel channel 1 gain control, incremental delay and vernier control to obtain the minimum reading on the true-reading rms voltmeter.

NOTE

This cancels amplification and delay differences, and the rms voltmeter indication is 2 times the resulting distortion.

Theory. Theory of this measurement concept is based on the definition of rms error:

$$e_{rms} = [e^2(t)]^{1/2} \quad . \tag{80}$$

True-readings rms voltage measuring devices give an indication proportional to an average power absorption over a period T_i, the instrument time constant. Specifically,

$$e_{rms}(t) = \sqrt{\frac{1}{T_i} \int_0^t e^2(\tau)\, \epsilon^{-k(t - \tau)}\, d\tau} \quad . \tag{81}$$

If the approximation is made that

$$\epsilon^{-k(t - \tau)} = 1, \; t - \tau < T_i$$

$$\epsilon^{-k(t - \tau)} = 0, \; t - \tau > T_i \quad ,$$

then

$$e_{rms}(t) = \left\{ \overline{[e^2(t)]_{T_i}} \right\}^{1/2} \quad . \tag{82}$$

Figure 16 is a block diagram of the system internal to the PN test set. For the case shown in the figure, the true-reading rms volmeter indicates

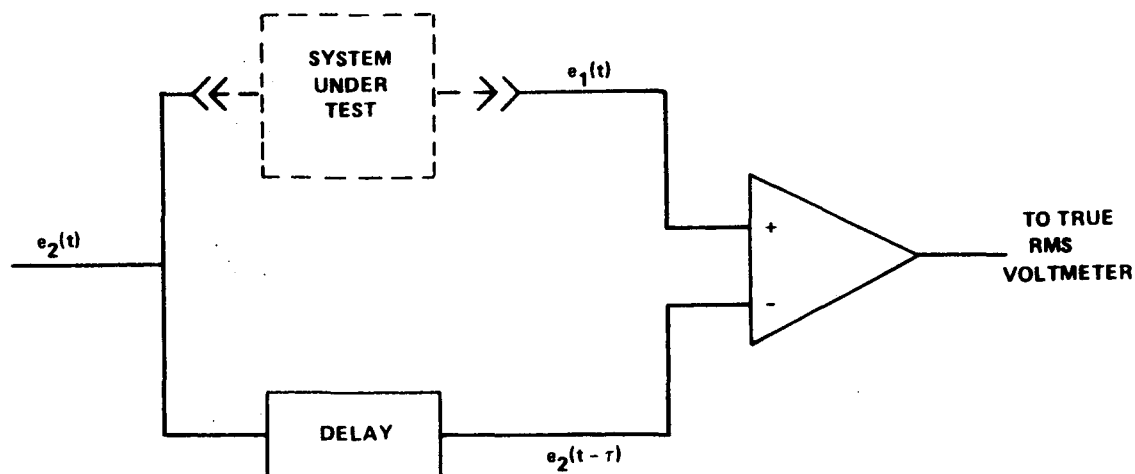$$e_{rms}(t) = \left\{ \overline{[e_1(t) - e_2(t - \tau)]_{T_i}^2} \right\}^{1/2} \tag{83}$$

Figure 16. Error detection section of the PN test set.

or

$$e_{rms}^2(t) = \overline{[e_1^2(t)]}_{T_i} + \overline{[e_2^2(t-\tau)]}_{T_i} - 2\overline{[e_1(t)\,e_2(t-\tau)]}_{T_i} \quad . \quad (84)$$

The PN test set output is a twofold amplification of the rms error; therefore, the rms meter reading equals $2e_{rms}^2$.

Record-Playback rms Error Measurement. Measurement of rms error due to distortion in a record-playback situation can be accomplished with the PN test set. Data from the system under test and the pseudonoise sequence is recorded and then played back to obtain the original data and measure the rms error.

Record Mode. The procedure for operating the PN test set in the record mode consists of the following steps:

    1.   Connect the test setup shown in Figure 17.

    2.   Place the PN test set controls in the following positions:

        a.   Mode switch to record.

        b.   Vernier delay switch to out.

        c.   Incremental delay switch to position 1.

    3.   Adjust the Ch 1 gain potentiometer to match the recorder interface requirements.

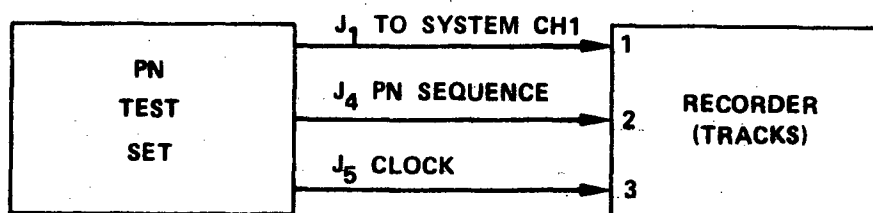   4.   Record data as required.

Figure 17. Test setup for recording.

Playback Mode. The procedure for operating the PN test set in the playback mode consists of the following steps:

1. Connect the test setup shown in Figure 18.

2. Place the mode switch in the playback position.

3. Activate the playback on the recorder.

4. Adjust the following PN test set controls to obtain the minimum rms error indication:

    a. Ch 1 gain.

    b. Incremental delay.

    c. Vernier delay.

NOTE

The rms voltmeter will read 2 times the rms error due to distortion in the record-playback process.

Time Delay Measurement. Average time delay in a telemetry-communication system may be computed by the following procedure.
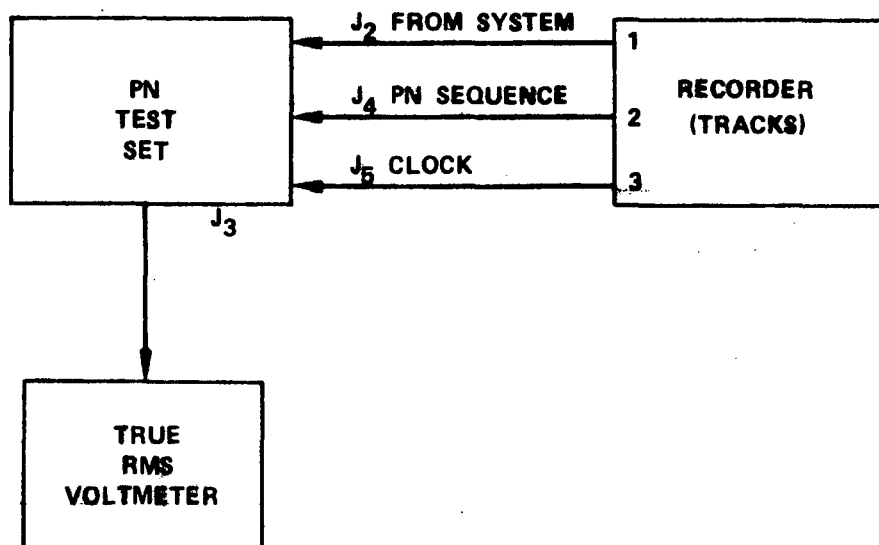

Figure 18. Test setup for playback.

1. Connect the test setup shown in Figure 19.

2. Using the procedure described in the section on real-time rms error measurement, measure the rms error.

3. Using a counter or an oscilloscope, measure the vernier time delay (in Ch 1) required to give this minimum rms error indication on the rms voltmeter.

The distance between negative-going edges of the two pulse-trains (start output and stop output) is the vernier time delay (d).

4. Compute the total time delay as

$$D_t = (k - 1/2) T + d$$

where k is the setting on the incremental delay switch and T is the clock period (22.2 μs for internal clock).

The setting of the incremental delay switch gives the additional delay in Ch 1, in steps of T (T equals 22.2 μs for internal clock operation).

When the vernier delay switch is the out position, D_t is equal to (k) T seconds.
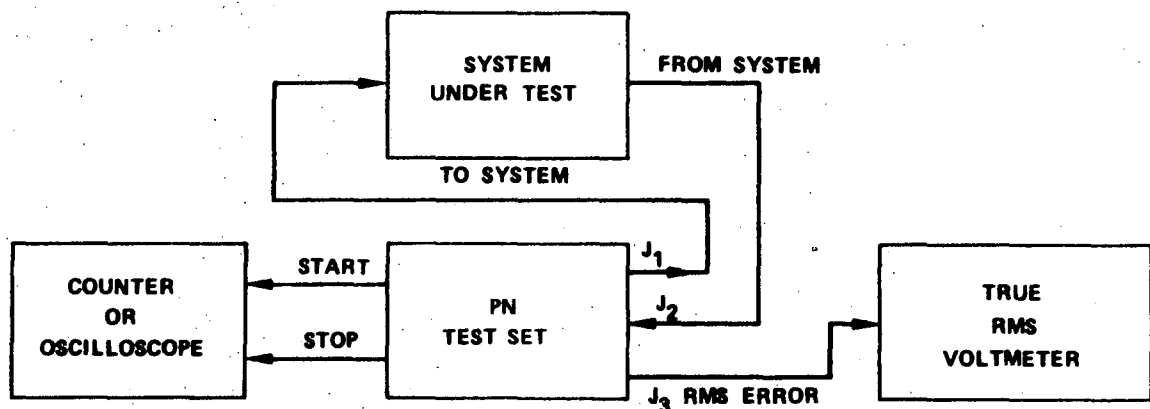

Figure 19.   Test setup for time delay measurement.

The measurements in the three previous subsections, the Ch 1 and Ch 2 dc offset potentiometers, mounted on card 6, need to be adjusted to obtain minimum rms error only when a dc reading true rms voltmeter is used. Most true rms voltmeters are ac reading only and do not include dc. The dc offset potentiometers are used to set the dc level of the data and reference signals.

Correlation Function Determination. Determination of the correlation function of a communication system may be accomplished by the following computation.

Since the correlation function for periodic waveforms is, by definition

$$Re_2 \, e_1 \, (\tau) = \frac{1}{T_0} \int_{-T_0/2}^{T_0/2} e_1 \, (t) \, e_2 \, (t - \tau) \, d\tau \quad , \qquad (85)$$

where T_0 is the basic period of the waveforms. Assuming that

$$T_i = T_0 \quad ,$$

then

$$e_{rms}^2 = \overline{[e_1^2 \, (t)]}_{T_0} + \overline{[e_2^2 \, (t - \tau)]}_{T_0} - 2Re_2 \, e_1 \, (\tau) \quad , \qquad (86)$$

or

$$Re_2 \, e_1 \, (\tau) = 1/2 \left(e_{1rms}^2 + e_{2rms}^2 - e_{rms}^2 \right) \quad . \qquad (87)$$

From the preceding equation, the correlation maximum occurs at the minimum rms error and by measuring system input, system output, and minimum rms error, the correlation of the system input and output is obtained. Remember that the PN test set measures $2e_{rms}$, and the value to be substituted into equation (87) is e_{rms}^2.

Impulse Response Determination. Determination of a telemetry communication system impulse response may be accomplished by the following procedure.

1. Determine the system correlation function in accordance with the instructions in this section.

2. Measure the system time delay (τ_{min}) in accordance with the instructions in this section.

3. For values of delay different from τ_{min}, measure $Re_2\, e_1\, (\tau)$ and obtain impulse response from equation (91).

Theory. Determine impulse response for the system with input, $e_i\, (t)$, and output $e_0\, (t)$.

1. The system correlation function is

$$Re_i\, e_0\, (\tau) = \int_{-\infty}^{\infty} e_i\, (t)\, e_0\, (t - \tau)\, dt \qquad (88)$$

also

$$Re_i\, e_0\, (\tau) = \int_{-\infty}^{\infty} Re_i\, e_i\, (t)\, h\, (t + \tau)\, dt \qquad (89)$$

where $h\, (t + \tau)$ is Green's function.

2. If the input is white noise, or looks like white noise to the system under test, then

$$Re_i\, e_i\, (t) = k\, \delta\, (0) \quad , \qquad (90)$$

and

$$\text{Re}_i \, e_0 (\tau) \; = \; kh (\tau) \quad . \tag{91}$$

Therefore, assuming the system under test is linear, the cross-correlation function is proportional to the system impulse response.

VI. ACCURACY ASSURANCE OF THE PN TEST SET

Interrelationship between Time Delay and Gain

In an analysis of communication system performance [4], the mean-square error between the input and output of a telemetry system has been expressed as

$$\sigma^2 (\tau, \, G) \; = \; \lim_{T \to \infty} \frac{1}{2T} \int_{-T}^{T} \, [e_i (t - \tau) - Ge_0 (t) - Gn_0 (t)]^2 \, dt \tag{92}$$

where $e_i (t - \tau)$ is the input signal delayed in time, τ is the time delay, G is the system gain, $e_0 (t)$ is the output signal exclusive of noise, and $n_0 (t)$ is the system noise. The waveform distortion is defined as the minimum of equation (92) which is obtained by proper selection of the variables τ and G. The values of τ and G that result in minimum error are defined as the average time delay, τ_0, and the average system gain, G_0. An important property to be considered in the measurement of waveform distortion, both analytically and experimentally, is that the parameter τ_0 can be determined independently of G_0. This property is illustrated by replacing equation (92) by the equivalent frequency domain expression (ignoring the noise term) given by

$$\sigma^2 (\tau, \, G) \; = \; \int_{0}^{\infty} s(\omega) \{1 - 2G \, A(\omega) \cos [\theta(\omega) + \omega\tau] + G^2 A^2(\omega)\} d\omega \quad , \tag{93}$$

where $s(\omega)$ is the input signal power density spectrum, $A(\omega)$ is the signal amplitude response, and $\theta(\omega)$ is the system phase response. The values of τ and G that minimize equation (93) are determined from the equations

$$\frac{\partial \sigma^2 (\tau, G)}{\partial \tau} = 0 \quad , \tag{94}$$

$$\frac{\partial \sigma^2 (\tau, G)}{\partial G} = 0 \quad . \tag{95}$$

Performing the integrations of equation (93) gives

$$0 = \int_0^\infty \omega s(\omega) A(\omega) \sin [\theta(\omega) + \omega \tau] \, d\omega \quad , \tag{96}$$

and

$$G = \frac{\displaystyle\int_0^\infty s(\omega) A(\omega) \sin [\theta(\omega) + \omega \tau] \, d\omega}{\displaystyle\int_0^\infty s(\omega) A^2(\omega) \, d\omega} \quad . \tag{97}$$

Hence, as noted from equation (96), solutions for τ may be obtained independently of G. If more than one solution is determined from equations (96) and (97), the desired solution is the one which results in minimum error.

The independence between τ and G is illustrated in Figure 20 where rms error is plotted as a function of time delay introduced into a band-limited random signal by an RC lowpass filter. The error is found to be a minimum at $\tau_0 = 0.046$ msec independent of the selection of G. The curve $G = 1.124$ represents the error for the average gain found in equation (97), while the minimum of the curve defines both the average time delay and the waveform distortion.
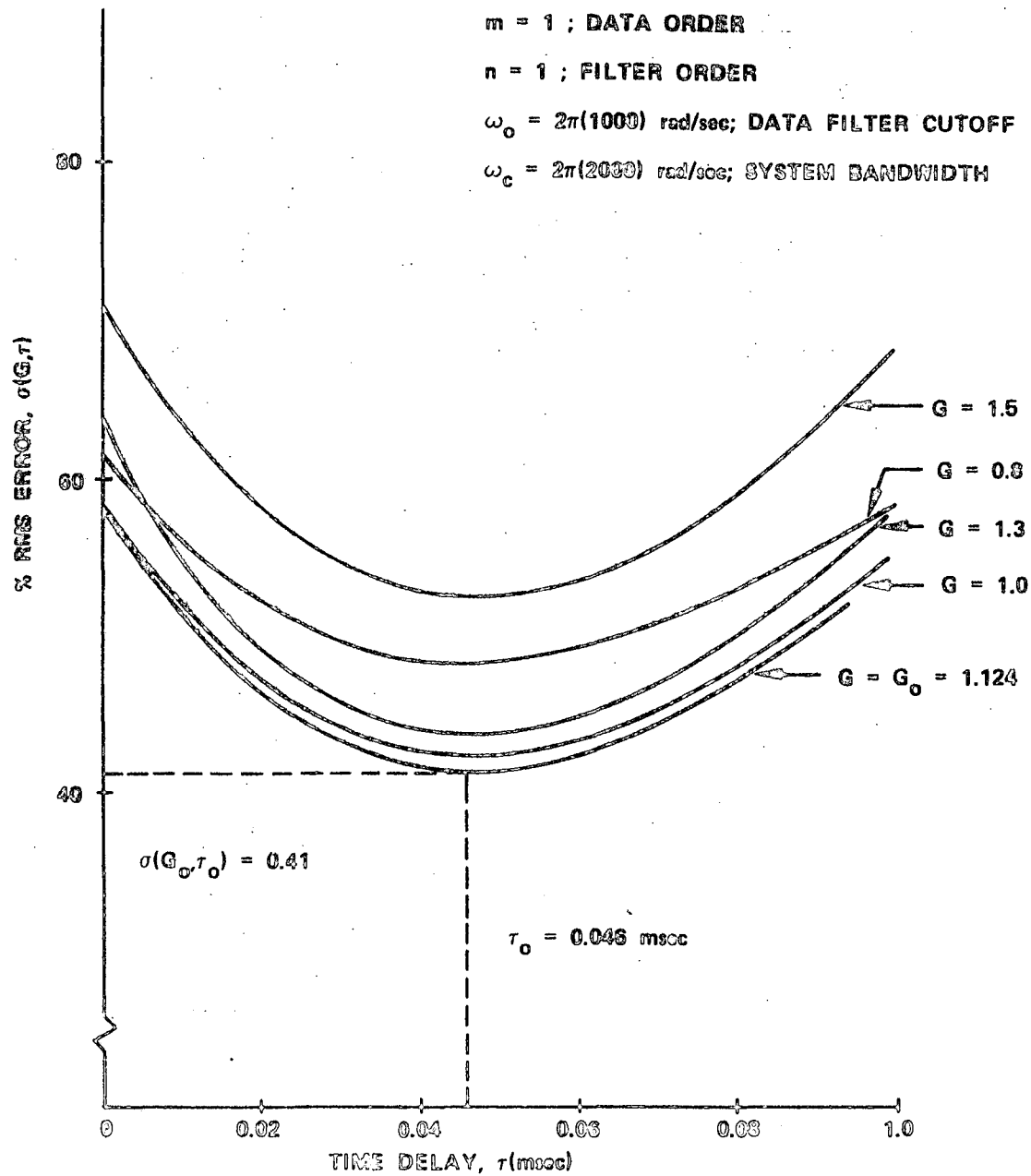
Figure 20. RMS error as a function of time delay introduced
into a band-limited random signal by an RC filter.

    The fact that the average time delay can be determined independently
of the system gain suggests that, in a laboratory test unit for measuring
waveform distortion, one should first seek to minimize the error by adjusting
the delay and then determine the absolute error minimum through adjustment

of the gain. The PN test set, with indepenently designed gain and delay capability, readily lends itself to this procedure. It should be mentioned that, in using this equipment, some adjustment back and forth between gain and time delay may be needed to achieve the desired measuring sensitivity. This would be the case where the initial gain setting is far from the desired setting, causing the error versus delay curve to be almost flat.

Experimental Accuracy Results

The total measuring accuracy of the PN test set has been examined in two ways. First, the noise floor of the unit was determined by simply connecting a coaxial cable between the system input and output terminals. It was found that the unit could be nulled to such a point as to insure less than 0.2 percent rms error with data signal levels ranging from 1.5 V p-p to 5 V p-p. Secondly, the distortion resulting from a more realistic blackbox configuration was determined and the measured values were compared with calculated results. The following information describes this second method for checking the accuracy of the PN test set.

The accuracy of the PN test set was checked against calculated data for several lowpass filters serving as blackboxes or test units. In general, the results substantiate the argument that the PN test set (in its use of determination of end-to-end rms errors) is functioning properly. Although all of the experimental values taken did not match the calculated values exactly, the variations were small, and explained.

There were several test filters (blackboxes with known characteristics) investigated with the PN test set. The basic setup used is the one shown in the block diagram in Figure 2.

In all analytical work, the calculated data were shaped from pure white noise which had a uniform density spectrum and a Gaussian amplitude probability density. All calculations were based on unmodified gains (i.e., if the unit under test changed the amplitude overall, this was not adjusted for minimum error).

Two characteristics of the PN sequence-generated data (as opposed to filtered white noise) should be explained.

First, consider Figure 21a. The calculated data were shaped from pure white noise and were assumed flat to ω_o, whereas the measured data (Fig. 21b) is 3 dB down at the ω_o. One would expect less error in the measured than in calculated as lower amplitudes were in the ω_o region.
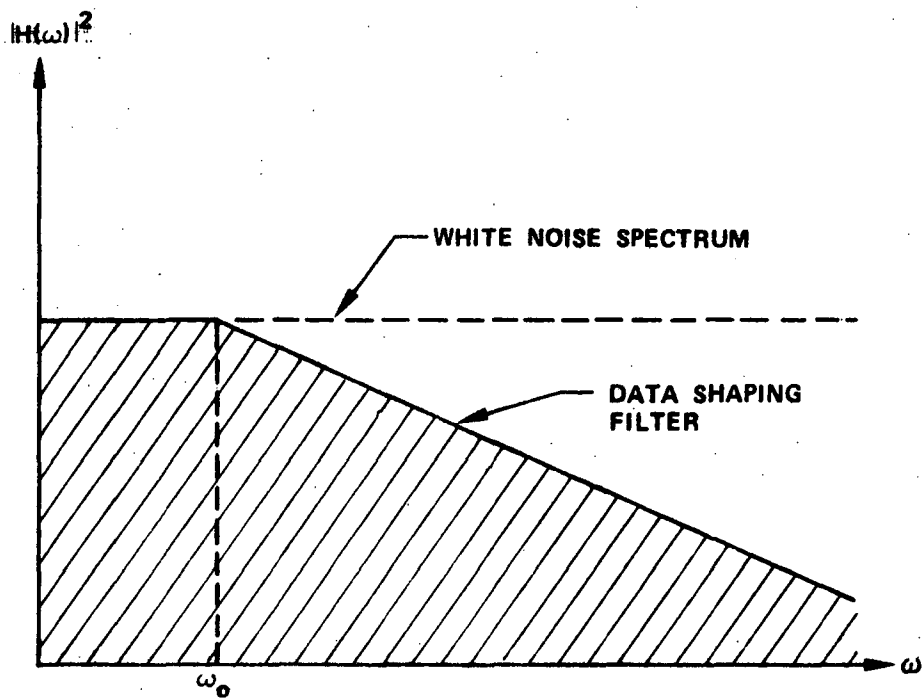
a. Calculated data spectrum.
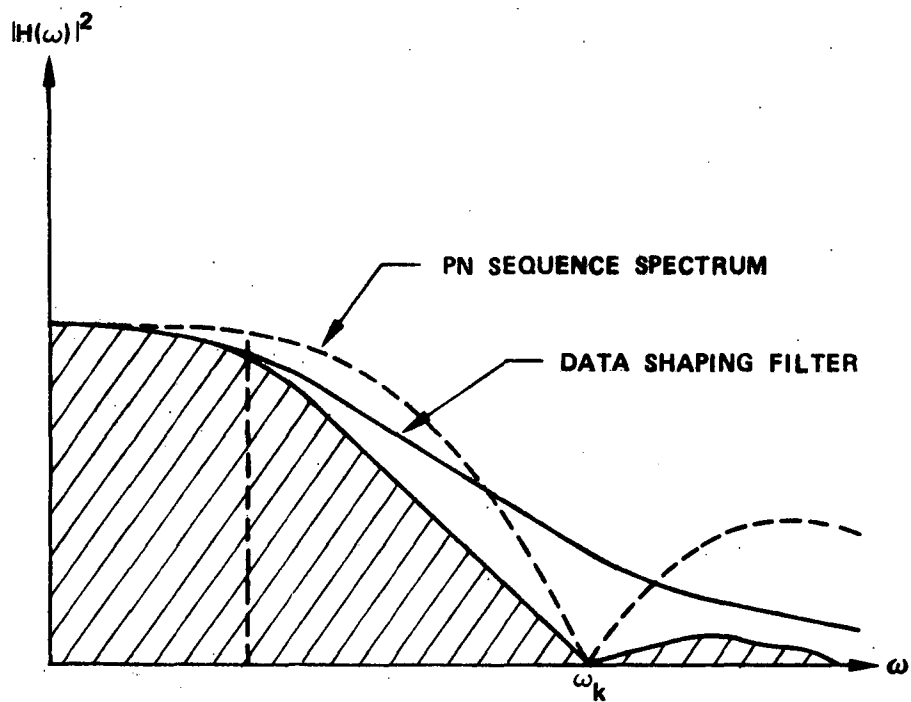
b. Filtered PN sequence spectrum.

Figure 21. Data spectra used for rms error measurements.

Second, the calculated data were shaped from pure white noise as in Figure 21a. Thus, the filtered data are assumed flat up to ω_o and is then attenuated at 6 m dB/octave (m is the number of poles in the filter) above cutoff. The PN sequence-generated data, from which the empirical data results were taken, only approximate the properties of white noise. In contrast to pure random noise, the PN sequence is actually periodic (refer to Figure 21b) and its spectrum nulls at integral multiples of ω_k, the clock frequency of the PN sequence generator.

As illustrated in Figure 21, the difference in spectral characteristics can be significant for ratios of $\omega_k/\omega_o = 20$ for a shaping filter with low stop-band attenuation. For example, with $\omega_k/\omega_o = 20$ and a filter attenuation rate of 6 dB/octave, the data in the vicinity of the first PN sequence null, ω_k, is only attenuated about 27 dB. Thus, for the calculated errors, data components exist at ω_k although attenuated 27 dB, while for the measured errors no data components exist at this frequency. Consequently, there is a difference between calculated and measured data in the vicinity of the PN sequence nulls as well as the difference noted near the filter cutoff frequency due to the characteristics of the approximated spectrum.

The way the data were taken was simply to vary ω_o of the test unit filter and take the rms error readings with the test setup as is shown in block diagram in Figure 2. High order (sixth) filters were used as well as lower (first) order filters in testing. Figure 22 shows the very close correlation of calculated and measured results for all filters when a third-order Butterworth data shaping filter pair was used. As one would expect, better correlation can be obtained by using higher order data shaping filters and blackbox or test filters (for the reasons explained above).

VII. TECHNICAL PROBLEMS ASSOCIATED WITH THE REALIZATION OF THE PN TEST SET

Two important technical problems surfaced in the design, construction, and evaluation of the PN test set. They included the extreme measurement accuracies required to tune the data filters to a mismatch of 0.1 percent or less, and a problem with skewing of the amplitude distribution of the pseudo-analog noise signal for large ratios of sequence clock frequency to data filter cutoff frequency.
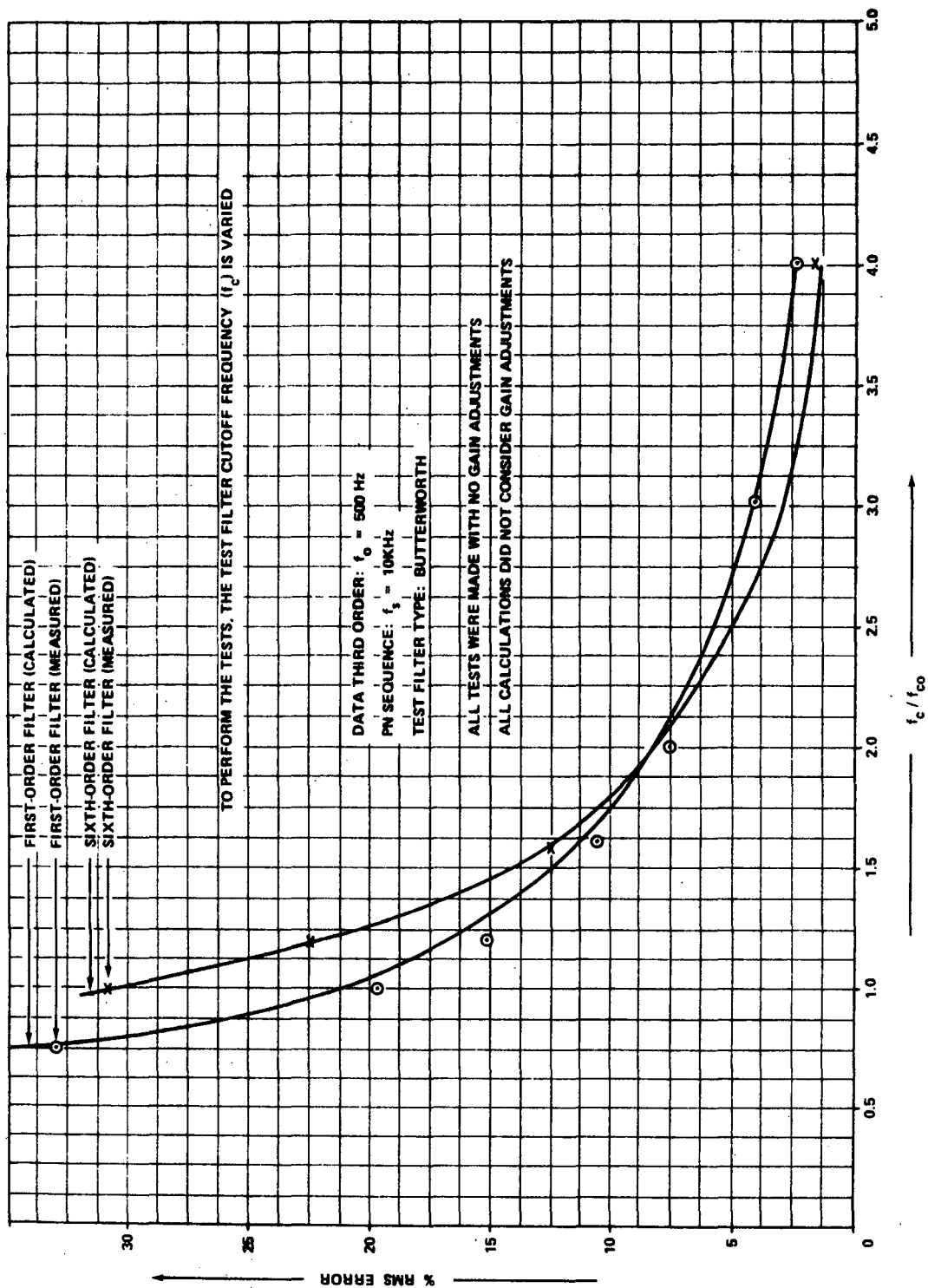
Figure 22. Plots for accuracy tests of PN test set.

Filter Match Problem

In the case of the filters, an initial passive design lowpass filter pair was matched to 0.4 percent rms error. An active design was developed and matched to better than 0.1 percent. Section IV gives the details of the active data filter set design and analysis.

For the purpose of developing an improved design procedure for matched data filters for pseudonoise testing, a filter component sensitivity analysis was performed. The analysis covered passive Butterworth and Chebyshev approximation type filters. The result was a mathematical procedure for isolating the error sensitivity of a component on comparison basis and for standardizing the tuning procedure. Section IV gives the results of the analysis and an example of its application.

Amplitude Distribution Skewing Problem

For the particular maximal length digital sequence generator designed into the PN test set, the amplitude distribution skewing problem was observed to occur for ratios of clock to data filter cutoff of 50 and above. Ideally, the distribution should approximate a normal curve as illustrated in Figure 23. This was found to be the case for the lower ratios of clock to filter cutoff frequency; however, for ratios of 50 and above the distribution was skewed as shown in Figure 24.
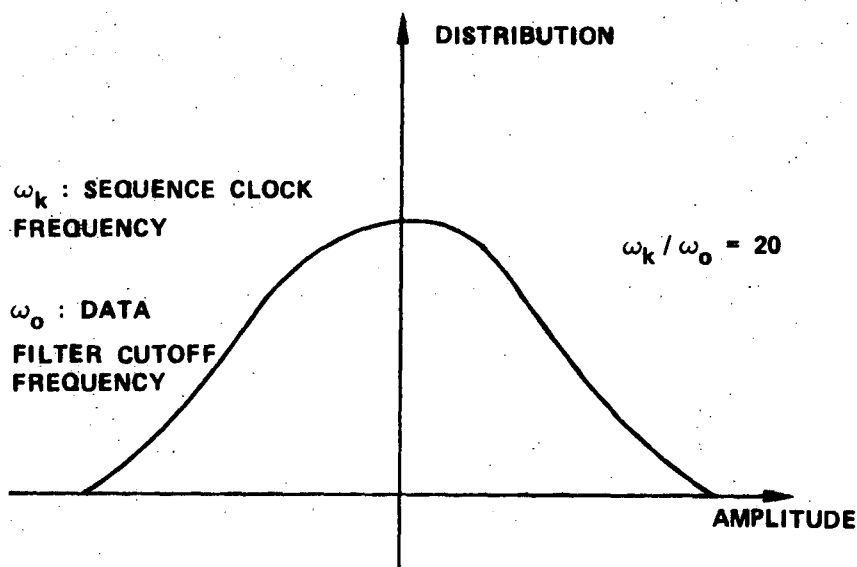

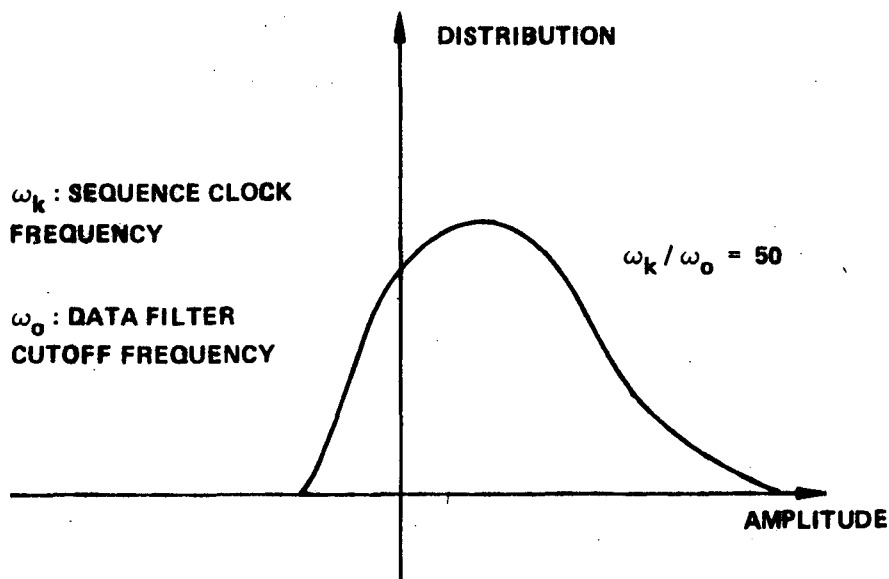Figure 23. Pseudorandom approximation to the normal distribution.

Figure 24. Skewed density function for large ratios of sequence
clock to data cutoff frequency.

An investigation of the causes of this skewing was undertaken in an
effort to correct the problem. A literature search revealed that R. P. Gilson
observed the phenomena in question and reported the results of an experimental
program concerning filtered maximum length sequences [5]. Gilson's report
confirmed that the skewing problem was basic to filtered ML sequences, and
not just a property of the particular ML generator in the PN test set. James
H. Lindholm reported the results of an analysis of the statistics of M-tuples
from ML sequences [6]. If the impulse response of the data filter is approx-
imated as a weighted sum of the last M-bits from the sequence generator,
Lindholm's results can be applied to the problem in question. Lindholm
showed that the third moment of the distribution of weights of M-tuples from
a maximum length sequence is related to the number of trinomials of order
M-1 or less that contain the sequence characteristic equation as a factor.
In the case of the PN test set, the M-tuple length corresponds to the ratio
of sequence clock to data filter cutoff frequency. The ML sequence generator
in the PN test set is a 20-stage unit with feedback from the 20th and 17th
stages. The sequence characteristic polynomial is

$$X^{20} + X^3 + 1 \tag{98}$$

and this polynomial apparently is a factor of many trinomials of order 50 or less. An investigation was made to determine if there are any sequence generators with approximately 20 stages that would have a characteristic polynomial that is a factor of few trinomials of order 50 or less. It was determined that the 23-stage sequence generator with feedback from stages 23, 17, 11, and 5 has such a characteristic ploynomial. A computer simulation of the filtered sequence, with a filter impulse response period of 60 clock periods, was performed. Figure 25 is the result of this simulation. The solid curve is the approximated normal distribution and the ● marks give the weights from the simulation. The approximation is satisfactory for the purposes of pseudonoise testing, and this sequence generator is planned for future models of the PN test set.
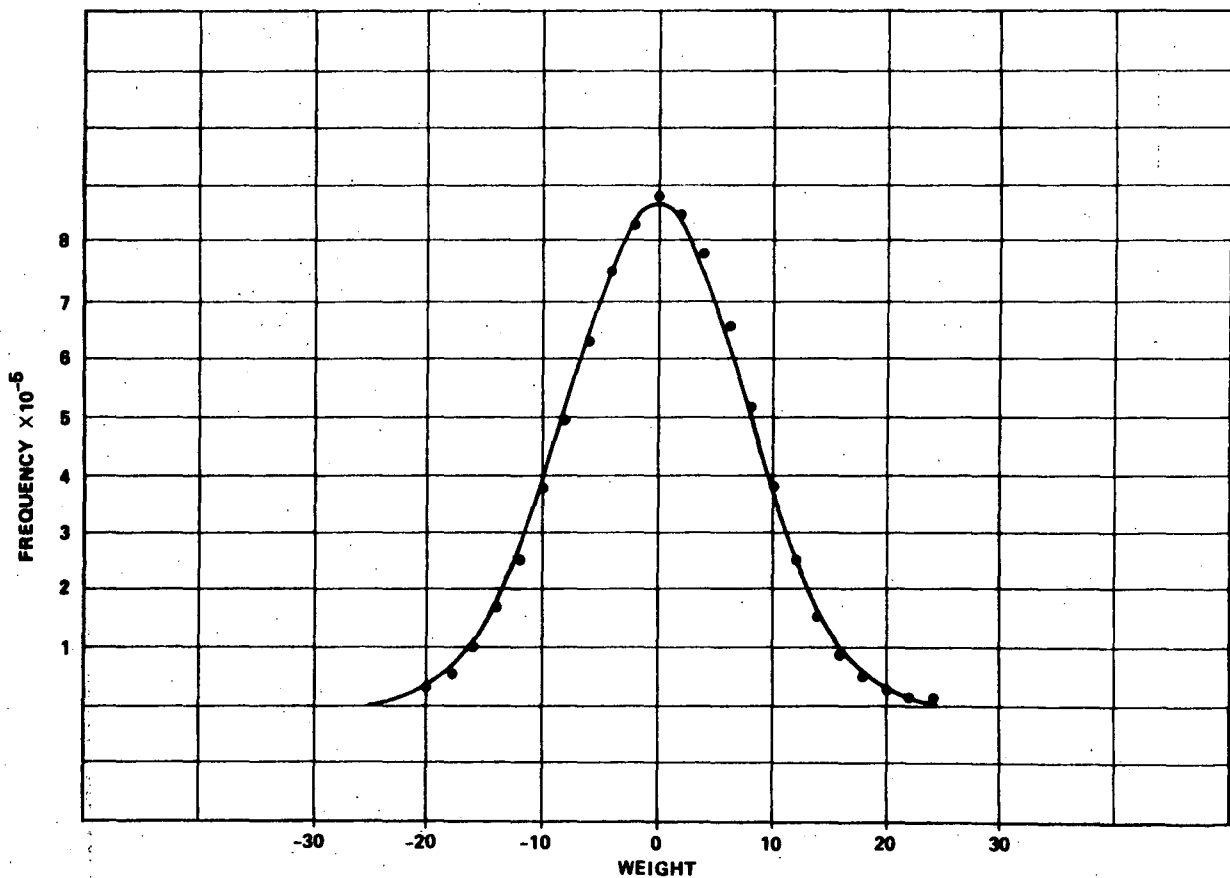

Figure 25. Normal probability and observed weights.

VIII. CONCLUSIONS

Although rigorous specification of the characteristics of filtered PN sequence data is apparently quite involved, the PN test set shows that a useful, pragmatic unit is available to provide rapid end-to-end rms error testing of communication systems. This unit uses filtered pseudorandom data and an analog error measuring approach to provide near-Gaussian, wideband data as a test signal. The test signal provided by the test set exercises the entire designed spectrum of the communication system under test.

This paper explains the concepts of system testing of both wideband random and simple, deterministic data as well as the problems involved in utilizing these digital and analog measuring techniques. The theory of PN testing is outlined and the description of the PN test set effectively shows how the theory is implemented. Its development has led to improved methods for fabricating and accurately matching filter pairs. Analytical and empirical tests were conducted to show that this unit can accurately measure system performance characteristics.

Two basic problems were noted during the project investigation: the need of a pragmatic method to overcome the extreme measurement accuracies needed to closely match the data shaping filter pairs, and the deviation of the data amplitude probability density distribution from the desired near-Gaussian distribution. Filter sensitivity analyses were used to overcome the filter fabrication problem and, while a specific PN sequence with a limited ratio of filter cutoff to clock frequency solved the immediate problem of a non-Gaussian distribution for the PN test set, additional investigations are being performed for more advanced data simulations for communication system testing.

APPENDIX A

EXPERIMENTAL METHODS (ANALOG AND DIGITAL) FOR MEASURING WAVEFORM DISTORTION

The basic intent of this appendix is to report two ways to perform end-to-end rms error testing on a system. Both schemes employ the idea of feeding a known signal into a system and comparing the system output with the known input to determine the degree of distortion. The question is how to data-load a system to get the most accurate test. The answer to this question must remain subjective until the specific system and its intended input data characteristics are known. However, to generalize somewhat, band-limited noise, limited to the test systems design data-handling capabilities, seems to be a reasonable check — primarily because it "exercises" the entire design spectrum simultaneously.

For the sake of discussion, one may first consider the two basic types of data with which to load a system to be tested, narrowband and wideband. By narrowband, one typically uses a sine wave signal (or perhaps sum of sine waves) and measures the delay and distortion of the system output compared to the input to get the induced distortion. Wideband data is meant to be data which will simultaneously exercise the system under test throughout its entire designed spectral range. It may be generated by a filtered noise source to produce the desired spectrum and a near-Gaussian amplitude probability density distribution, a sum of sine waves, or a filtered PN sequence.

Waveform distortion in a telemetry system or subsystem may be defined as the minimum mean-squared difference between the input signal and the output signal. Constant gain or delay between the input and output is not considered as error; therefore, an efficient means of eliminating these factors from the error calculation must be devised. Mathematically, the error is defined as

$$\overline{\sigma^2(t)} = \lim_{T \to \infty} \frac{1}{2T} \int_{-T}^{T} [e_i(t - \tau) - Ge_0(t) - Gn_0(t)]^2 \, dt \tag{A-1}$$

where $e_i(t-\tau)$ is a delayed replica of the input signal, $e_0(t)$ is the output signal, and $n_0(t)$ is the output noise. To determine the waveform distortion, the delay and the gain G must be that of the system under test.

Two methods, and the basic reason for this appendix, for measuring waveform distortion are presented. The first approach follows the general ideas of Shepertycki and uses analog techniques for computing the error. The second approach employs digital techniques for determining the error.

Analog Method

Figure A-1 outlines a method for measuring signal distortion first proposed by Shepertycki [7]. The test signal is generated as a discrete pseudorandom digital waveform clocked through a series of shift register elements so that each element has an output delayed by exactly one clock period relative to the preceding element. The test signal, simulating the wideband data, is formed by passing the binary output from stage one of the pseudorandom signal source through a selected lowpass filter, called the data filter. A delayed replica of the pseudorandom signal is applied to a second data filter, identical to the first, and then compared with the communication system output in a differential amplifier. The two pick-off points for generating $e_i(t)$ and $e_i(t-\tau)$ are placed such that the delay between them is
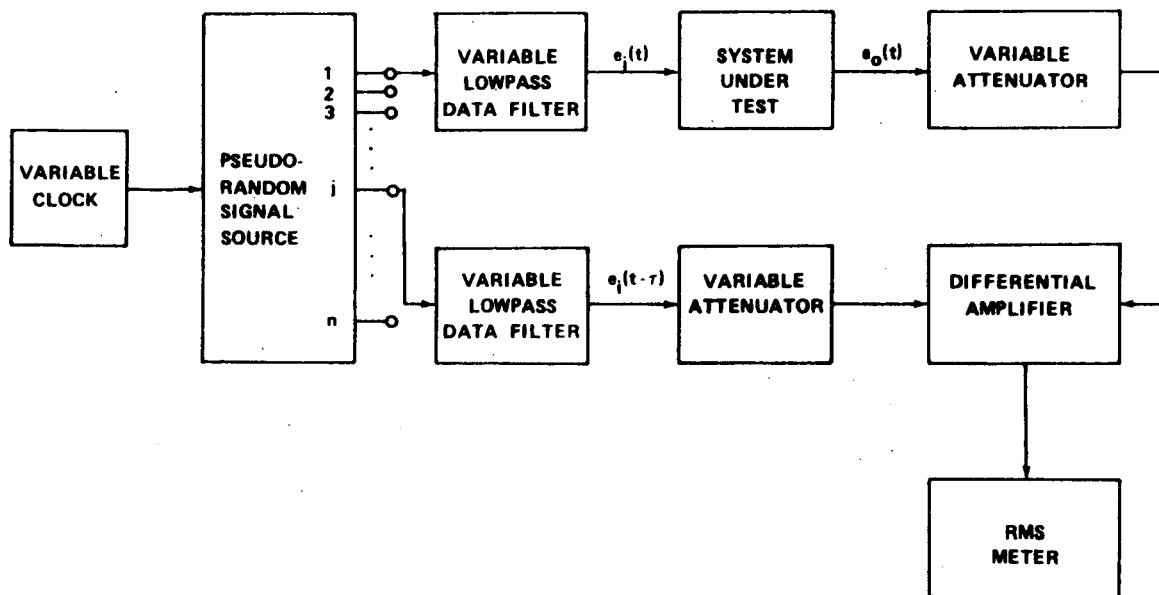

Figure A-1. Analog technique for measuring signal distortion.

approximately equal to the delay through the communication system. The clock frequency is then varied for fine adjustments of the delay.

Both delay and gain are adjusted to minimize the differential amplifier output. This minimal output represents the waveform distortion introduced by the communication system and any residual errors contributed by the test apparatus. The degree of residual errors is easily evaluated by repeating the measurement with the communication system removed.

Application of the analog technique requires careful selection of clock frequency and the pseudorandom signal generator. In general, the clock frequency should be made at least 10 times greater than the 3 dB bandwidth of the data filter. This insures that the data spectrum shape is a function primarily of the frequency characteristics of the data filter. The number of stages in the PN sequence generator and delay circuitry should be chosen so that the total time delay available in the generator is at least equal to the delay in the system under test.

The equipment involved with the analog technique has the advantage of being compact and relatively inexpensive. On the other hand, some undesirable characteristics associated with this technique are (1) the data filters must be matched very accurately, which in practice has been difficult to achieve, and (2) the analog computing devices are inherently nosiy and subject to drift and frequency distortions.

Some additional problems may be encountered in maintaining the desired signal characteristics. Provided the bandwidth of the analog shaping filter is much less than the clock frequency, the test signal possesses a flat frequency spectrum out to the bandwidth of the filter and (supposedly) has a Gaussian amplitude probability density distribution. Unfortunately, in many applications involving this method of noise generation, the output becomes skewed for large clock frequency/data filter bandwidth ratios.

Digital Method

With some complexity, sample-and-hold circuits can be used to provide the necessary time delay for measuring signal distortion. A block diagram of a unit employing these so-called digital techniques is shown in Figure A-2. In this system, time delay is adjusted continuously by variation of a clock frequency. The clock is used to drive an input scanner (time-division multiplexer) and an analog-to-digital (A/D) converter. The input scanner is composed of ring counter elements that drive analog gates leading
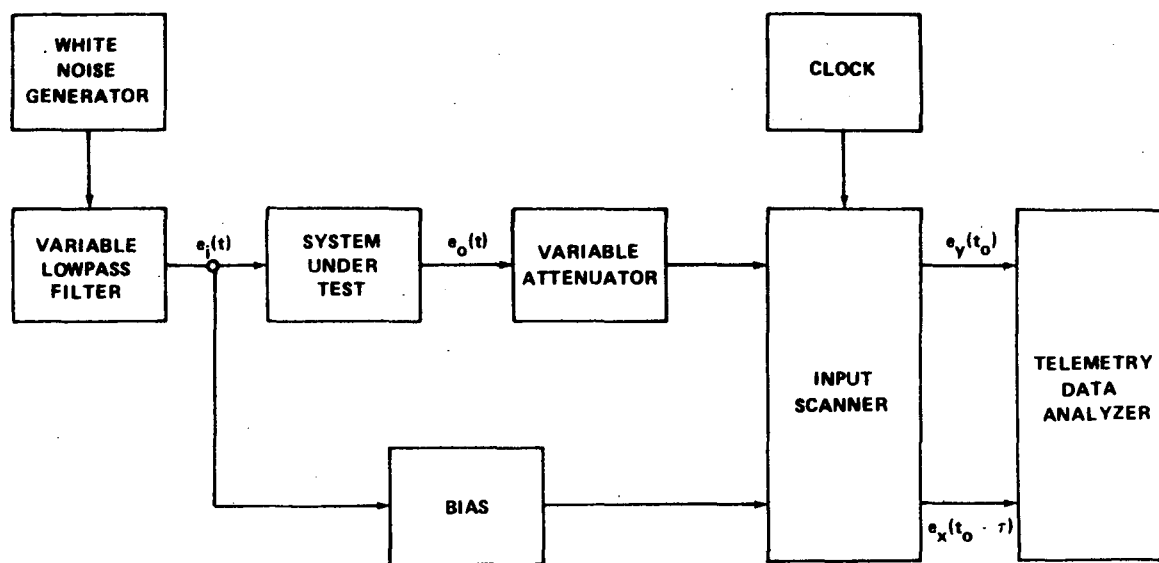
Figure A-2. Digital technique for measuring signal distortion.

to the sample-and-hold circuitry of a digital-to-analog (D/A) converter. The time delay between any two ring-counter elements is an integral number of clock periods so that a direct relationship between time delay and clock period is established. Thus, the clock period is easily converted to units of time delay.

In the unit outlined in Figure A-2, $E_y(t_0)$ is a sampled version of the communication system output and $E_x(t_0 - \tau)$ is the corresponding delayed version of the input signal. Both outputs appear in the form of a 10-bit PCM serial wavetrain. The Telemetry Data Analyzer[1] synchronizes to this wave-train, separates the two data samples, and performs the necessary operations to determine the error. The number of samples taken for a calculation depends on the required accuracy and may be selected as desired.

Comparison of Results

It should be noted that any analog device may be inserted into the "system" section of the test configurations in Figures A-1 and A-2 and its error determined. To establish some correlation between these suggested

---

1. The Telemetry Data Analyzer is special purpose equipment designed for Astrionics Laboratory to provide, among other things, a means of rapidly performing sampled rms end-to-end error evaluations.

error measurement techniques and analytical results, the error resulting from a 6-pole Butterworth lowpass filter was measured. With the analog technique, the pseudorandom output from a 20-stage generator was passed through a 3-pole Butterworth lowpass filter to form the data source. With the digital technique, white noise shaped with a 3-pole Butterworth lowpass filter provided the data source. In Figure A-3, rms error is expressed as a percent of rms input signal strength. It is seen that theoretical and experimental results agree closely, giving a great degree of confidence in both error measurement techniques.

The techniques described have been successfully used to measure single-channel and multi-channel distortion CBW/FM telemetry systems. As expected, the results offered a high degree of reproducibility, leading to substantially the same results with each successive measurement.
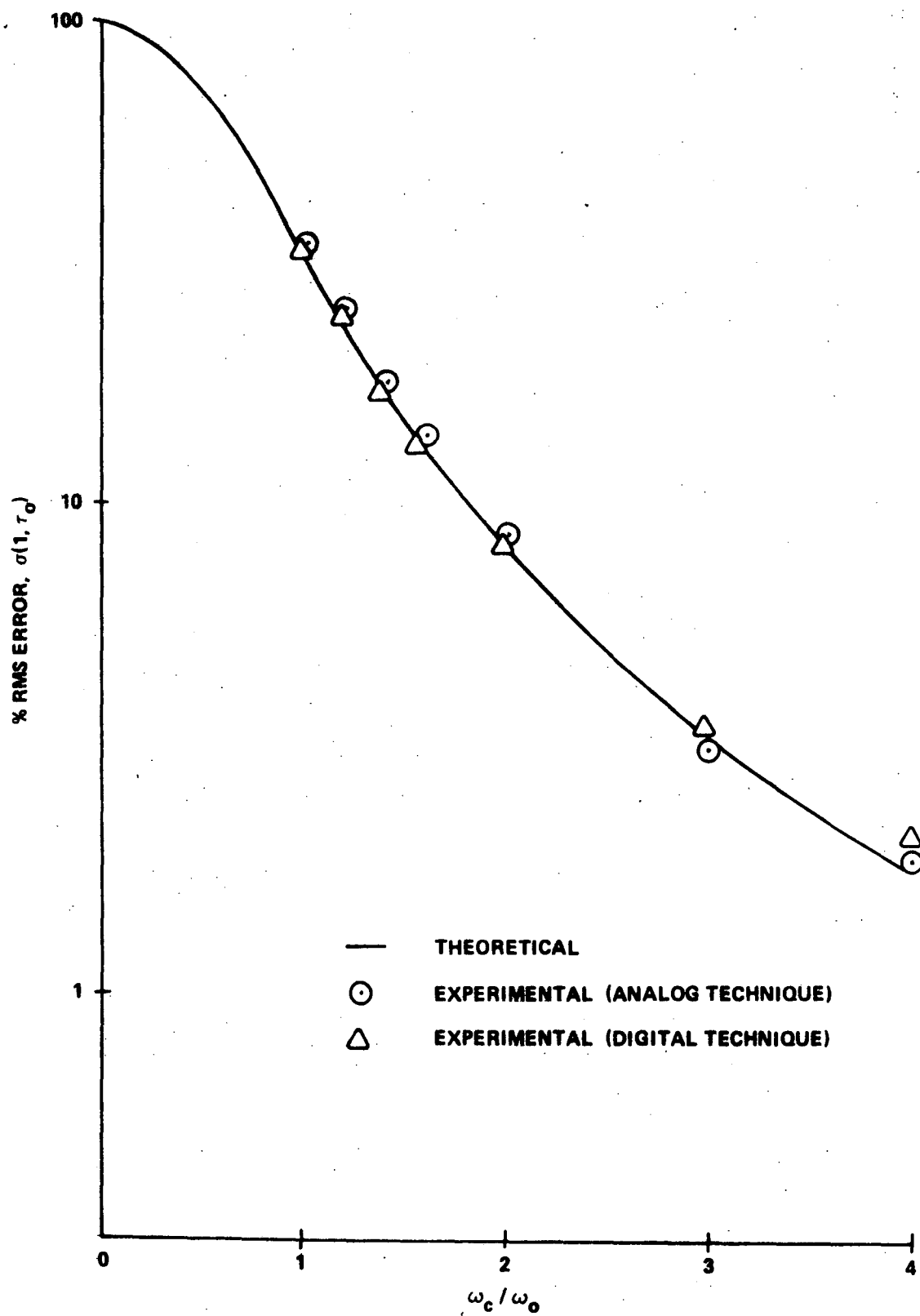
Figure A-3. Distortion of third-order band-limited data by a six-pole Butterworth lowpass filter.

APPENDIX B

EVALUATION OF A MATCHED LOWPASS FILTER SET

This appendix gives the results of an evaluation of a pair of matched lowpass filters (manufactured by Kappa Networks, Carteret, New Jersey). The purpose of the evaluation was to determine if the quality of the filter match was sufficient to qualify the filters for application in the pseudonoise test set.

Figure B-1 gives a standard schematic for lowpass filters of the type evaluated. The filter specifications were as follows:

Filter Order — Third

Type Response — Lowpass, Butterworth

Load Impedance — R_L = 5000 ohms

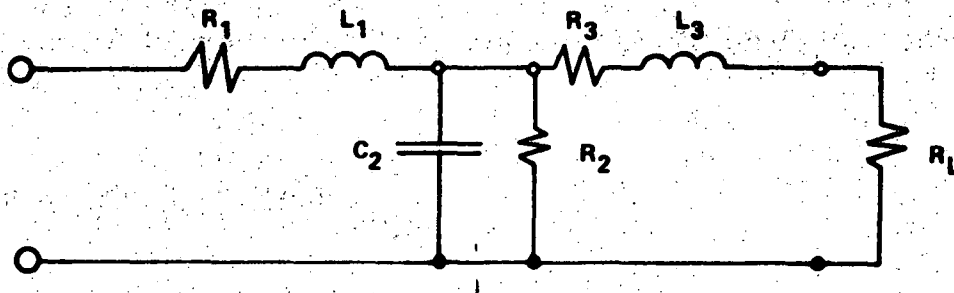Match Quality — 0.05 percent

Figure B-1. Filter schematic.

Figure B-2 indicates the procedure used by Kappa in checking the match quality of the filters during tuning. With a sinusoidal input signal, the filter set was checked throughout its frequency range of operation for a normalized difference signal of 0.0005. The frequency range of operation was taken to be about three times the 3 dB cutoff frequency. The assumption was made that if

$$f_1(\omega) - f_2(\omega) \leq 0.0005 \, f_1(\omega) \qquad\qquad \text{(B-1)}$$

for all, where $f_1(\omega)$ is filter number 1 output and $f_2(\omega)$ is filter number 2 output, then

$$\int_0^\infty [f_1(\omega) - f_2(\omega)] \, d\omega \leq 0.0005 \int_0^\infty f_1(\omega) \, d\omega \quad , \qquad \text{(B-2)}$$

or

$$\frac{\int_0^\infty [f_1(\omega) - f_2(\omega)] \, d\omega}{\int_0^\infty f_1(\omega) \, d\omega} \leq 0.005, \qquad\qquad \text{(B-3)}$$

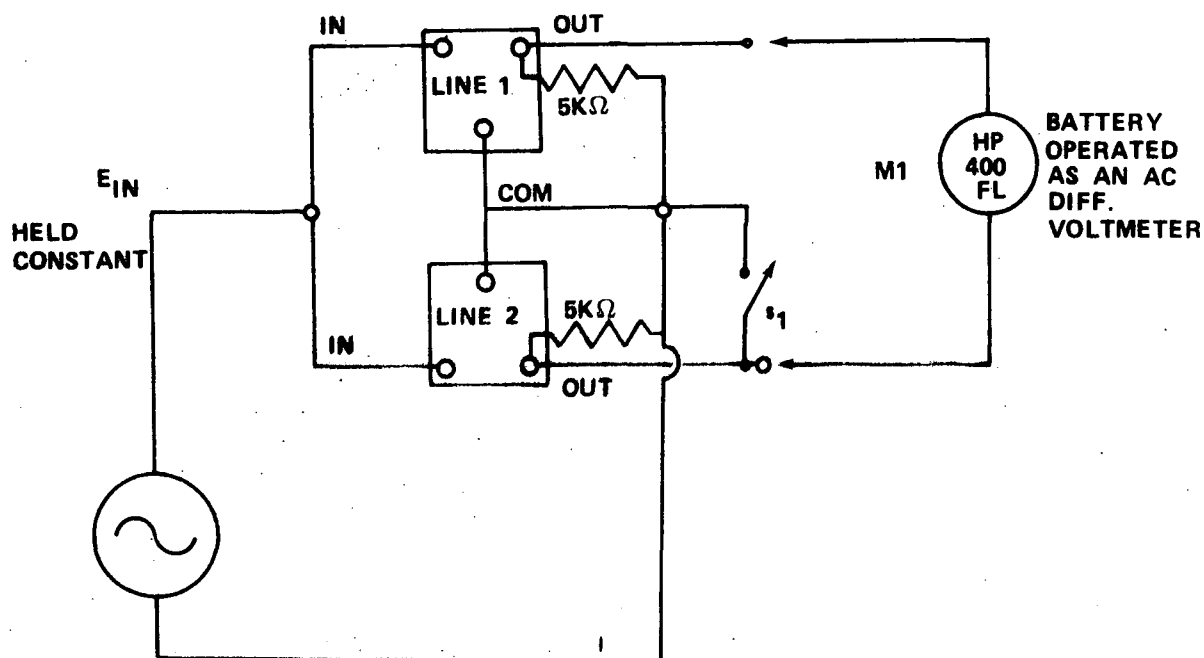and the filter set would meet the desired match quality specification.

Figure B-2. Kappa's test procedure.

To check the final match quality of the delivered filter set, an input drive signal with an approximately uniform spectrum was used.

Figure B-3 gives the schematic of the test circuit. The drive signal was a pseudorandom digital sequence with a bit rate of 6 kHz. The sequence length was 1023 bits, and this resulted in an input data spectrum with a harmonic component spacing of 5.86 Hz.

The filter test procedure was as follows:

1. Close switch s_1 and adjust the gain control to confirm the ability of the difference amplifier to null to better than 0.01 percent normalized.

2. Open switch s_1 and adjust the gain to the best null. Measure the rms value of the difference signal V_d.

3. Close switch s_2 and measure the rms value of the reference signal V_r.

4. Calculate match quality in percent, (V_d/V_r) 100 percent.

The measured match quality was not quite as good as the 0.05 percent specified and was found to vary slightly with the magnitude of the input signal. Typical measurements were:

V_r	V_d	Match Quality
0.95	0.001	0.11%
0.66	0.0008	0.12%

Even though the measured match quality was not as good as the specified value of 0.05 percent, it may still be within the limits allowable in the pseudonoise test set.
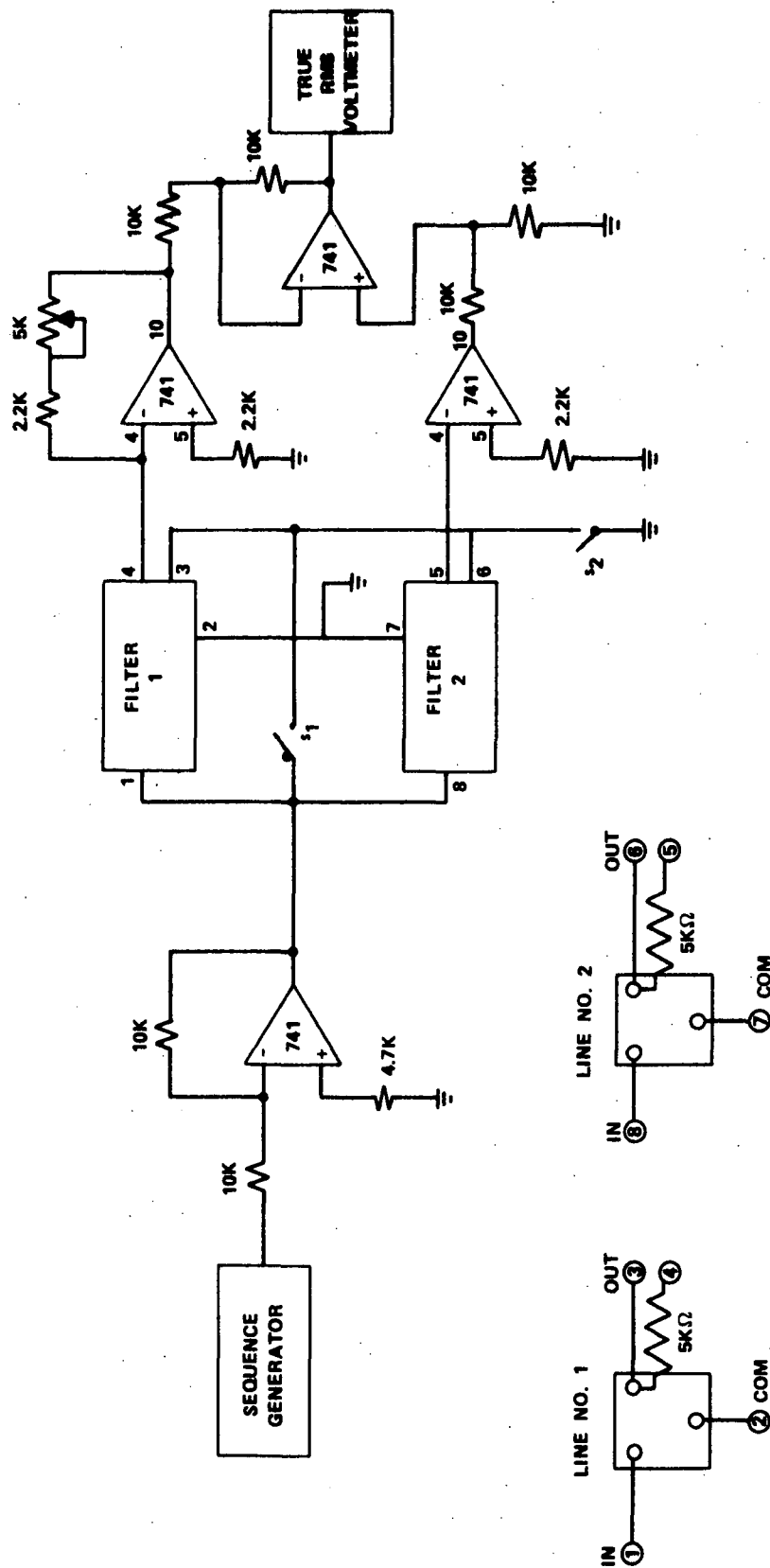
Figure B-3. Filter test scheme.

REFERENCES

1. Gussow, Sidney and Weathers, Glenn: Computer-Aided Filter Design Manual. NASA SP-3049, 1969, pp. 19-35.

2. Gussow, Sidney: Analysis and Synthesis of Active Quadratic Filter Networks for Telemetry Applications. Thesis, University of Alabama in Huntsville, 1969.

3. Weathers, Glenn and Parikh, Uday: Filter Sensitivity Analysis by an RMS Method. Report SP-275-0577, Sperry Rand Corp., Space Support Division, pp. 2-36.

4. Salter, W. E.: A Study of the Major Sources of Distortion in AM-Baseband Telemetry System and Techniques for Optimum Baseband Design. Dissertation, University of Alabama, 1972, p. 24.

5. Gilson, R. P.: Some Results of Amplitude Distribution Experiments on Shift Register Generated Pseudo Random Noise. IEEE Transactions on Electronic Computer, December 1966, pp. 926, 927.

6. Lindholm, James H.: An Analysis of the Pseudo Randomness Properties of Subsequences of Lang M-Sequences. IEEE Transactions on Information Theory, vol. T-14, no. 4, July 1968, pp. 569-576.

7. Shepertycki, T. H.: Telemetry Error Measurements Using Pseudo Random Signals. IEEE Transactions on Space Electronics and Telemetry, September 1964, pp. 111-115.

THE PSEUDONOISE TEST SET: COMMUNICATION SYSTEM'S PERFORMANCE EVALUATION BASED UPON RMS ERROR TESTING

By G. R. Wallace, S. S. Gussow,
W. E. Salter, and G. D. Weathers

The information in this report has been reviewed for security classification. Review of any information concerning Department of Defense or Atomic Energy Commission programs has been made by the MSFC Security Classification Officer. This report, in its entirety, has been determined to be unclassified.
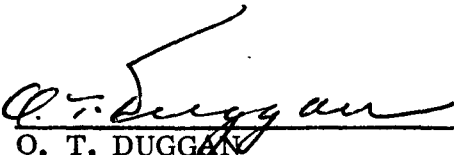
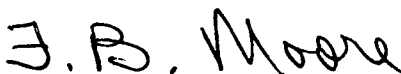This document has also been reviewed and approved for technical accuracy.

_____
W. B. THRELKELD
Chief, Telemetry, Test, and Analysis Section

_____
ROBERT EICHELBERGER
Chief, Telemetry and Data Technology Branch

_____
O. T. DUGGAN
Chief, Instrumentation and Communication Division

_____
F. B. MOORE
Director, Astrionics Laboratory

DISTRIBUTION

INTERNAL

DIR
DEP-T

PD-DO-EC
Mr. Arsement

S&E-DIR

S&E-R-DIR
Dr. Johnson

S&E-DIR
Dr. Haeussermann

S&E-ASTR-DIR
Mr. Moore

S&E-ASTR-C
Mr. Swearingen

S&E-ASTR-G
Mr. Mandel

S&E-ASTR-I
Mr. Duggan
Mr. Frost

Mr. Atherton
Mr. Eichelberger
Mr. Coffey
Mr. Lawson
Mr. Threlkeld
Dr. Wallace (20)
Dr. Salter (Sperry 4)
Mr. Gussow (Sperry 4)
Mr. Weathers (Sperry 4)
Mr. Frederick (Sperry 4)

S&E-ASTR-M
Mr. Boehm

S&E-ASTR-R
Mr. Taylor

S&E-ASTR-ZX
A&TS-MS-H
A&TS-MS-IL (8)
A&TS-MS-IP (2)

A&TS-PAT
Mr. L. D. Wofford, Jr.

A&TS-TU
Mr. Winslow (15)

EXTERNAL

Scientific and Technical Information
    Facility (2)
P. O. Box 33
College Park, Maryland 20740
Attn: NASA Representative (S-AK/RKT)

Professor R. O. Pettus
College of Engineering
University of South Carolina
Columbia, South Carolina 29208

Professor D. Irwin
Dept. of Electrical Engineering
College of Engineering
Auburn University
Auburn, Alabama 36830

Professor M. A. Honnell
Dept. of Electrical Engineering
College of Engineering
Auburn University
Auburn, Alabama 36830

Professor E. R. Graf
Dept. of Electrical Engineering
College of Engineering
Auburn University
Auburn, Alabama 36830